

DM haloes in the fifth-force cosmology

Wojciech A. Hellwing,^{a,b,c} Marius Cautun,^d Alexander Knebe,^e
Roman Juszkiewicz,^{a,f} and Steffen Knollmann^e

^aInstitute of Astronomy, University of Zielona Góra, ul. Lubuska 2, 65-001 Zielona Góra, Poland

^bInterdisciplinary Center for Mathematical and Computational Modeling, University of Warsaw, ul. Pawińskiego 5a, 02-106 Warsaw, Poland

^cInstitute for Computational Cosmology, Department of Physics, Durham University, Science Laboratories, South Rd, Durham DH1 3LE, UK

^dKapteyn Astronomical Institute, University of Groningen, P.O. Box 800, 9747 AV Groningen, The Netherlands

^eGrupo de Astrofísica, Departamento de Física Teórica, Módulo C-8, Facultad de Ciencias, Universidad Autónoma de Madrid, 28049 Cantoblanco, Madrid, Spain

^fNicolaus Copernicus Astronomical Center, ul. Bartycka 18, 00-716 Warsaw, Poland

E-mail: pchela@icm.edu.pl, cautun@astro.rug.nl

Abstract. We investigate how long-range scalar interactions affect the properties of dark matter haloes. For doing so we employ the ReBEL model which implements an additional interaction between dark matter particles. On the phenomenological level this is equivalent to a modification of gravity. We analyse the differences between five ReBEL models and Λ CDM using a series of high resolution cosmological simulations. Emphasis is placed on investigating how halo properties change in the presence of a fifth force. We report that the density profile of ReBEL haloes is well described by the NFW profile but with mean concentrations from 5% to a few times higher than the standard Λ CDM value. We also find a slight increase of the halo spin for haloes more massive than $5 \times 10^{11} h^{-1} M_{\odot}$, reflecting a higher rotational support of those haloes due to scalar forces. In addition, the dark matter haloes in our models are more spherical than their counterparts in Λ CDM. The ReBEL haloes are also more virialised, with a large difference from Λ CDM for strong fifth forces and a much smaller change for weak scalar interactions.

Keywords: cosmology, dark matter, haloes, large-scale structure, phenomenology

ArXiv ePrint: [1111.7257](https://arxiv.org/abs/1111.7257)

¹Corresponding author.

Contents

1	Introduction	1
2	Scalar-interacting DM: the ReBEL model	2
2.1	The phenomenological model and modified gravity	5
2.2	The growth of structures in the ReBEL model	6
3	N-body simulations	7
3.1	The effects of baryons	9
4	Results: Statistical properties of the halo populations	9
4.1	Density profiles	10
4.2	Spin & halo rotation	13
4.3	Shapes and geometry	17
4.4	Virialisation	20
5	Conclusions	22

1 Introduction

The Λ CDM model has proven capable of explaining a tremendous amount of observational data. In the era of precision cosmology, from both an observational and modelling perspective, we are left with a more and more detailed picture of the evolution of the universe. This precisely measured history can be used to impose constraints not only on the cosmological parameters (e.g. [1–4]) but also on the nature of dark matter (DM) [5–10].

The strong relationship between DM characteristics and the emerging large scale structure (LSS) has been investigated in detail (e.g. [11–19]). Most of the attention has focused on large scale linear structures and on the properties of highly non-linear small-scale objects like haloes and galaxies. There still remains a considerable amount of unanswered questions with respect to the physical nature of DM. Due to the great difficulties involved in the direct detection of DM particles in Earth-based experiments, astrophysical observations still form the most important source of information on the nature and properties of DM particles.

The currently established Λ CDM paradigm has some still unsolved problems whose solutions may reveal additional details about DM. On galaxy scales, these answered questions involve the precise quantitative understanding of galaxies rotation, the central cusp of DM haloes and explaining the observed rich population of thin disk dominated spiral galaxies that contrasts the Λ CDM high merger and accretion rate at low redshifts (for an excellent discussion refer to [20, 21]). On Megaparsec scales, the most interesting and well known problem involves the void phenomenon, strongly emphasised by Peebles in [22]. It concerns the apparent discrepancy between the number of observed dwarf halos in voids and that expected from Λ CDM simulations.

While there are clear discrepancies between observations and the predictions of Λ CDM cosmological simulations, there is not a clear consensus if these problems are due to our inability to simulate the universe in enough details or because of yet unknown physics present in the dark sector. This motivated us to investigate the effects of additional DM physics on formation and evolution of structures in the cosmos. Studies of exotic new physics in the DM sector are also important from a

high-energy physics point of view. The results of modified DM models when compared with current cosmological observations can be used to impose constraints and narrow down the possible DM candidates.

One of such possible CDM paradigm modifications, formulated on the grounds of supersymmetry and string theory, has been proposed and developed by Gubser, Peebles and Farrar [23–26]. It consists of cold DM that, in addition to gravity, interacts by exchange of scalar particles. This model, dubbed ReBEL (*daRk Breaking Equivalence principLe*), has shown the potential to solve some of the galaxy formation and evolution problems discussed above. The difference between ReBEL and the standard CDM model consists in the additional interaction between DM particles, a so-called “fifth force”, which acts exclusively on DM and has a limited range. Studies employing N-body simulations of the ReBEL model [20, 27–32] and similar models of coupled DM and dark energy (DE) [33–35] have shown that this class of models reproduces the observed large scale structure of the universe (e.g. the 1D power spectrum of the Ly- α forest galaxies or the power spectrum from the SDSS galaxy survey¹). At the same time, it was shown that the ReBEL model introduces new effects, potentially positive, to the process of structure formation on galactic scales.

The recent years have seen several works that studied the effects of modified DM and DE models [36–47]. These have been motivated by recent observations posing even more challenges to the standard Λ CDM cosmology. Some of the new puzzles include an observed offset between baryonic and DM in clusters [48] and reports on very massive superclusters seen at high redshifts [49–51]. These have important constraints and implications for both Λ CDM and modified DM and DE theories [52–54]. The new observations have made the nature and properties of DM and DE a hotly discussed and debated topic.

In this paper we study the impact of the ReBEL model and its form of modified gravity on the internal properties of DM haloes. We do so by performing a suite of N-body simulations using ReBEL DM physics that we compare with the results of the standard Λ CDM cosmology. This work comes into the international and multidisciplinary collective effort taken to further understand and study the nature of DM and its implication for cosmology.

This paper starts with the theoretical formulation and the physics of the ReBEL model which are presented in section 2. This is followed by section 3 where we describe the numerical experiments that we performed to study the formation and evolution of DM haloes. The DM halo comparison is presented in section 4. Finally we end with section 5 where we give our conclusions and final remarks.

2 Scalar-interacting DM: the ReBEL model

In this section we will briefly present, using [23, 24, 27] as reference, the fundamental ideas and properties of the ReBEL model discussed in this paper.

We consider a picture in which there exist an additional long-range force - different than gravity - that acts only on DM particles. Such a force arises due to the interactions between DM particles and some underlying background scalar field ϕ . Such an interaction can be expressed formally as:

$$\mathcal{S} = - \int |\phi| ds, \quad \text{or} \quad (2.1)$$

$$\mathcal{S} = \int \sqrt{-g} d^4x (i\bar{\psi}\gamma\partial\psi - \phi\bar{\psi}\psi). \quad (2.2)$$

¹Sloan Digital Sky Survey - <http://www.sdss.org/>

The idea of long-range interactions appearing due to exchange of massless scalar particles has a very long history. Nordström derived the classical form of Eq. (2.1) in 1913 [55]. This interaction is equivalent, in the limit of small de Broigle lengths, to the form given in Eq. (2.2) which was introduced by Yukawa [56].

Within the framework of quantum field theory there are arguments stating that it is very unlikely for any scalar field to escape from obtaining a large mass ($\gg H_0$), which would make any model with a scalar field particularly useless for cosmology. However, additional work on the grounds of the string theory suggest that there is a possibility for a scalar field to maintain low mass.

In the beginning of the second half of the 20th century Pascual Jordan and Robert Dicke presented a few papers exploring the physics of the scalar-tensor gravity implementing above action integral defined for particles in the Einstein frame [57–59].

In 1990 Damour *et al.* [60] noticed that the tight empirical constraints that we have for long-range scalar interactions in the baryon sector allow for existence of such interaction with significant strength in the dark sector. Modern considerations along this line of thought appear abundantly in the literature of this subject [61–73].

We now focus on the model described in detail by Gubser and Peebles in [23, 24]. Let us consider at least two different species of DM particles which interact, in addition to gravity, by a scalar field. This additional interaction is dynamically screened by the presence of light particles coupled by a Yukawa-like factor to the scalar field. The generic Lagrangian for such a scenario is given by:

$$\mathcal{L} = \frac{1}{2}(\partial\phi)^2 + \bar{\Psi}_s i \not{\nabla} \Psi_s + \bar{\Psi}_+ i \not{\nabla} \Psi_+ + \bar{\Psi}_- i \not{\nabla} \Psi_- - y_s \phi \bar{\Psi}_s \Psi_s - (m_+ + y_+ \phi) \bar{\Psi}_+ \Psi_+ - (m_- - y_- \phi) \bar{\Psi}_- \Psi_- , \quad (2.3)$$

where $\not{\nabla}$ is the operator in Feynman slashed notation:

$$\not{A} \equiv \gamma^\mu A_\mu . \quad (2.4)$$

Here γ^μ are Dirac's gamma matrices and the equation is written using the Einstein summation convention. The constants m_\pm and y_\pm are both positive. The fermions Ψ_\pm are non-relativistic DM while the additional species of light particles Ψ_s consist of the screening particles.

The action for the two particle species takes the form:

$$\mathcal{S} = \int \sqrt{-g} d^4x \phi_{,i} \phi^{,i} / 2 - \sum_{\text{particles}} \int [m_+(\phi) ds_+ + m_-(\phi) ds_-] , \quad (2.5)$$

where the symbol $_{,i}$ denotes a partial derivative. The DM particles carry effective scalar charges Q :

$$Q_+ \equiv \frac{dm_+}{d\phi} < 0, \quad Q_- \equiv \frac{dm_-}{d\phi} > 0, \quad \frac{d^2 m_\pm}{d^2 \phi} \geq 0 , \quad (2.6)$$

which in general are conserved for non-relativistic phenomena². The field ϕ will undergo quasistatic relaxation towards equilibrium, yielding larger values in the regions where the (+) particles dominate and smaller values in aggregations of the (-) particles. Thus, a particle with positive (+) charge will be attracted towards regions with large ϕ values because it has a lower energy $m_+(\phi)$. Similarly negatively charged particle (-) will be attracted to the regions with small ϕ values. This behaviour implies that particles with the same charge attract each other while particles of different kinds repel.

²In general the scalar charges are not conserved for interactions at relativistic energies. Additionally, the scalar charge of DM trapped in a black holes is lost.

This basic scenario is similar to the so-called multi-coupled dark energy models (see e.g. [74–77]). However, in this study we investigate the most basic and simple model of the ReBEL cosmology, in which there is only one heavy species of scalar particles acting effectively as DM. The basic scheme that we assume admits for a relatively simple numerical implementation, that, at the same time, allows us to study a model that can be understood as a generic fifth-force model. In this context, our simplest ReBEL scenario is more generic than the phenomenologically rich multi-coupled dark energy models. Hence further we assume that there are two species of the DM particles which satisfy:

$$m_{DM} = m - y\phi, \quad m_s = y_s\phi, \quad \text{and} \quad y\bar{n} < y_s\bar{n}_s \quad (2.7)$$

where m_{DM} is the mass of heavy particle species (effectively the mass of a DM particle), m_s labels the mass of the screening particles, and \bar{n} & \bar{n}_s are the corresponding number densities of this particles. The scalar field ϕ has relaxed to quasistatic equilibrium, for which $m_s \sim 0$. Thus, the screening particles are relativistic and generate the potential:

$$V_s = \sum_{\text{particles}} \int y_s \phi ds \simeq \int d^4r y_s \phi n_s \langle \sqrt{1 - v^2} \rangle. \quad (2.8)$$

This implies that:

$$\frac{\delta V_s}{\delta \phi} = y_s n_s \langle \sqrt{1 - v^2} \rangle \simeq \frac{y_s^2 \bar{n}_s}{\varepsilon_s} \phi, \quad \text{with: } \varepsilon_s = \frac{y_s \phi}{\sqrt{1 - v^2}}. \quad (2.9)$$

Where the ε_s labels the averaged energy of a screening particle and $\langle \sqrt{1 - v^2} \rangle$ is the mean velocity of the screening particles (when $c = 1$). The equation for the scalar field now takes the form:

$$\nabla^2 \phi = \frac{\phi y_s^2 \bar{n}_s}{\varepsilon_s} - y n(\mathbf{r}, t). \quad (2.10)$$

The above equation is consistent with an effective damping of the scalar field ϕ by the term:

$$r_s = \sqrt{\frac{\varepsilon_s}{y_s^2 \bar{n}_s}} \quad [\text{Mpc}] \quad (2.11)$$

which we call the screening length³. Making use of the r_s definition, we rewrite the scalar field equation as:

$$\nabla^2 \phi = \frac{\phi}{r_s^2} - y n(\mathbf{r}, t). \quad (2.12)$$

Let us analyse this last equation in more detail. The last term describes the non-relativistic particles in a hydrodynamic approximation. The term ϕ/r_s^2 appears here [25], because the source term of the ϕ field for a particle with velocity v contains factor $ds/dt = \sqrt{1 - v^2}$ and for quasistatic configurations of the ϕ the energy of the screening particles ε_s (see Eq. (2.9)) is nearly independent of their location. Elimination of the $\sqrt{1 - v^2}$ in favor of ε_s leads to the equation for the screening length (2.11). The ε_s energy does not depend on time since it is constant, thus due to the expansion of the Universe it has to scale like $\varepsilon_s \propto a(t)^{-1}$. Taking into account that $n_s \sim a(t)^{-3}$, we conclude that the screening length grows like $r_s \sim a(t)$. Hence it is a constant in comoving coordinates.

³This term is equivalent to the cut-off length in a Yukawa-like potential

At small distances ($r \ll r_s$) the scalar field generated by a single DM particle has the value $\phi = y/4\pi r$. Taking into account that the force exerted by this field on another DM particle equals to the negative gradient of the mass $m - y\phi$, we obtain:

$$\mathbf{F}_s = y\nabla\phi. \quad (2.13)$$

Which clearly shows that two DM particles are attracted by the scalar interaction:

$$F = \frac{y^2}{4\pi r^2} \quad \text{for } r \ll r_s. \quad (2.14)$$

Two DM particles also interact gravitationally. This leads us to define the β parameter which is the ratio of the scalar to gravitational force strength between two identical DM particles. This parameter is given by:

$$\beta = \frac{y^2}{4\pi G m^2} \quad \text{for } r \ll r_s. \quad (2.15)$$

Setting $\beta \sim \mathcal{O}(1)$ gives us scalar interactions which have a magnitude comparable to that of gravity. For distances much larger than the screening length this scalar interactions fade away to zero. Hence the formula for the total force exerted on two DM particles can be splitted into two limiting cases:

$$F_{DM} = (1 + \beta)F_N \quad \text{for } r \ll r_s, \quad (2.16)$$

$$F_{DM} = F_N \quad \text{for } r \gg r_s. \quad (2.17)$$

To summarise, we are dealing with a model of DM which, in addition to gravity, interacts by means of a scalar field. The model introduces two free parameters β and r_s , which are sufficient for a full phenomenological description.

2.1 The phenomenological model and modified gravity

Following the earlier work of [27, 28], we study the ReBEL model using its phenomenological parametrisation. In this approach we model the scalar interactions appearing in the dark sector as effectively modified gravity. This is clear when we write the modified potential between two DM particles as:

$$\Phi(\mathbf{r}) = -\frac{Gm}{r}h(r) = \Phi_N h(r) \quad (2.18)$$

with

$$h(r) = 1 + \beta e^{-r/r_s}. \quad (2.19)$$

Here G is the Newton gravitational constant, \mathbf{r} marks the separation vector between particles and Φ_N is the pure Newtonian potential. As we have shown in the previous section, our model is described by two parameters: β - the dimensionless factor measuring the ratio between scalar and gravitational forces and r_s - the screening length expressed in Mpc. Elementary considerations from string theory [23, 24, 27] give crude estimations for the values of the parameters as:

$$\beta \sim \mathcal{O}(1), \quad r_s \sim 1\text{Mpc}. \quad (2.20)$$

The potential given in Eq. (2.18) gives rise to a modified force-law between two DM particles:

$$F_{DM} = -G\frac{m^2}{r^2} \left[1 + \beta \left(1 + \frac{r}{r_s} \right) e^{-\frac{r}{r_s}} \right] = F_N \cdot F_s(\beta, \gamma), \quad (2.21)$$

$$\text{where: } \gamma \equiv \frac{r}{r_s}, \quad F_s(\beta, \gamma) = 1 + \beta(1 + \gamma)e^{-\gamma}. \quad (2.22)$$

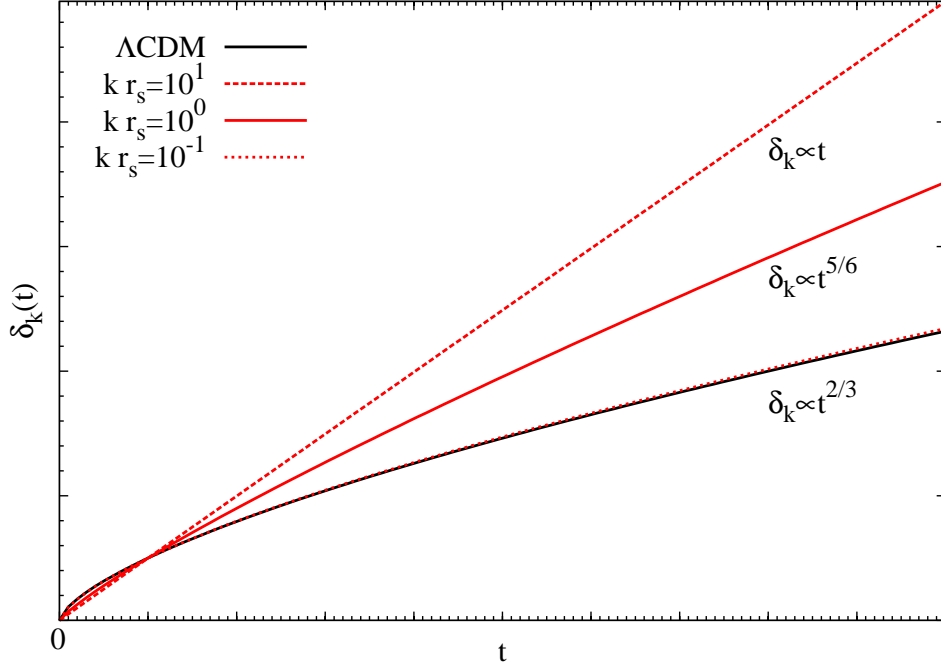


Figure 1. Growth of the Fourier modes of density perturbations in the linear regime during the matter dominated era as predicted by Eq. (2.25). Solid black line depicts the Λ CDM model with $\delta_k \propto t^{2/3}$ for all values of k . Solid, dotted and dashed red lines mark the growth of density perturbations in the ReBEL model for $\beta = 1$ and at three different values of $r_s \cdot k$. Both axes have arbitrary units.

Where the F_s term measures the force deviations from the usual Newtonian gravity and F_N marks the Newtonian force. We call F_s the ReBEL factor. For $\beta = 0$ or $\gamma \gg 1$ we will get $F_s \rightarrow 1$, hence $F_{DM} \rightarrow F_N$ and we recover the standard Newton force law.

Equations (2.18)-(2.22) yield a simple phenomenological description of the ReBEL addition to the CDM model.

2.2 The growth of structures in the ReBEL model

Now that we defined a phenomenological approximation to the ReBEL DM physics (Eqs. 2.18-2.21), we can analyse how the presence of the scalar interactions affects structure formation. In doing so we limit ourselves to the matter dominated epoch since that period is especially important for galaxy formation and evolution. We use linear perturbation theory to study the growth of density perturbations in the regime $\delta \lesssim 1$. Because the ReBEL model changes the dynamics of DM only on scales small compared to the Hubble scale, ReBEL does not affect the global evolution of the scale factor described by the Friedman equations. Due to the modified force law given by Eq. (2.21), the Poisson equation for the DM component of the ReBEL model reads:

$$\vec{\nabla} \times \Phi = 0, \quad \nabla_{\vec{r}}^2 \Phi = 4\pi G\rho \left(1 + \beta e^{-|\vec{r}|/r_s}\right) \quad (2.23)$$

To better understand the effects of the modified force, we linearise this equation together with the Euler and continuity equations in the limit of small perturbations in δ , v_p and ϕ (the density, peculiar velocity and gravitational potential perturbations around a smooth background) [78]. The evolution of the density perturbation for the matter-dominated epoch, which is well described by the Einstein-de

Sitter universe with $\Omega = 1$, is given by:

$$\ddot{\delta}_k + \frac{4}{3t}\dot{\delta}_k = \frac{2}{3t^2} \left[1 + \frac{\beta}{1 + (kr_s)^{-2}} \right] \delta_k \quad (2.24)$$

which, for convenience, we write in Fourier space. The growing mode solution for this equation is [27]

$$\delta_k \propto t^\alpha, \quad \alpha = \frac{1}{6} \sqrt{25 + \frac{24\beta}{1 + (kr_s)^{-2}}} - \frac{1}{6}. \quad (2.25)$$

For $kr_s \ll 1$ we get $\alpha = 2/3$, thus Fourier modes with $k \ll r_s^{-1}$ grow exactly in the same manner like in the standard Λ CDM model. On the other hand perturbations on scales smaller than characteristic screening length ($k \gtrsim r_s^{-1}$) grow faster than in the standard model. For example in the particular case with $\beta = 1$ and $kr_s \gg 1$ we have $\delta_k \propto t$. A comparison of the time evolution of Fourier density modes between Λ CDM and ReBEL is shown in Figure 1. The figure gives the growth of density fluctuations δ_k in a ReBEL $\beta = 1$ model for three modes satisfying $kr_s = 10, 1$ and 0.1 . The figure shows that structure formation is enhanced and accelerated in ReBEL compared to the Λ CDM case on scales $\lesssim r_s$. Moreover, different Fourier modes experience different time evolution, from $\delta_k \propto t$ for $kr_s \ll 1$ to $\delta_k \propto t^{2/3}$ for $kr_s \gg 1$. Faster growth of the small-scale density ! perturbations in ReBEL make these modes to cross into non-linear regime ($\delta \gg 1$) quicker, which should result in earlier DM haloes formation and virialisation. This was already shown to some extent in [20, 30].

3 N-body simulations

Table 1. The parameters describing our N-body simulations. The β and r_s [h^{-1} kpc] depict the values of the ReBEL model free parameters used in a given simulation run, L [h^{-1} Mpc] is the box size, z_{ic} is the redshift of the initial conditions, Ω_m and Ω_Λ are the dimensionless DM and DE density parameters (at $z = 0$), σ_8 is the r.m.s. of the density fluctuations smoothed on $R = 8h^{-1}$ Mpc, h is the dimensionless Hubble parameter, m_p is the mass of a single DM particle in units of $10^8 h^{-1} M_\odot$, ε [h^{-1} kpc] is the force resolution, l [h^{-1} kpc] labels the mean inter-particle separation and N_p gives the total number of DM particles.

Simulation	β	r_s	L	z_i	Ω_m	Ω_Λ	σ_8	h	m_p	ε	l	N_p
LCDM	-	-	32	1100	0.3	0.7	0.8	0.7	0.203	6	62.5	512^3
B005RS500	0.05	500	32	1100	0.3	0.7	0.8	0.7	0.203	6	62.5	512^3
B01RS500	0.1	500	32	1100	0.3	0.7	0.8	0.7	0.203	6	62.5	512^3
B05RS500	0.5	500	32	1100	0.3	0.7	0.8	0.7	0.203	6	62.5	512^3
B05RS1000	0.5	1000	32	1100	0.3	0.7	0.8	0.7	0.203	6	62.5	512^3
B1RS1000	1.0	1000	32	1100	0.3	0.7	0.8	0.7	0.203	6	62.5	512^3

As mentioned earlier, string theory considerations provide a crude estimate for the values of the two free parameters: $\beta \sim 1$ and $r_s \sim 1h^{-1}$ Mpc [27, 28]. According to this, in this paper we explore four possible values of the $\beta = 0.05, 0.1, 0.5 \& 1.0$ and two values of the screening length parameter $r_s = 0.5 \& 1h^{-1}$ Mpc. We label the corresponding simulations runs as LCDM, B005RS500, B01RS500, B05RS500, B05RS1000, B1RS1000, where B stands for β and RS marks the r_s parameter. The LCDM run is the one with $\beta = 0$ (i.e. no scalar forces) and corresponds to the standard cosmological model Λ CDM.

All simulations were started with the same initial conditions at $z_{ic} = 1100$. We need to adopt such a high starting redshift, since, in general, the scalar forces in our scenario start acting on DM shortly after recombination. This set-up allows for a proper treatment of any non-linearities that may

arise in early Universe due to scalar forces. Earlier ReBEL studies have usually assumed $\beta \geq 0.5$, neglecting that scalar forces arise already in the early universe. Therefore, one should understand the previous results of [27–30, 32] in a purely phenomenological way, where the value of the β parameter describes just a toy-model approximation to the ReBEL picture. Allowing the scalar forces to start acting at very high redshift (e.g. $z \approx 1100$) produces more pronounced effects at $z = 0$. By studying these effects we found that models with $\beta \geq 0.5$ and $r_s \geq 500h^{-1}$ kpc values produce cosmic density fields characterised by a higher $\sigma_8(z = 0)$ value than the fiducial Λ CDM run. For example, the B1RS1000 model has a σ_8 value 10% higher than the Λ CDM cosmology. The higher variance of the density field, and the value of the σ_8 parameter in particular, is the direct outcome of the fifth-force that enhances DM clustering. This effect was already shown and studied for the ReBEL model [28, 32] as well as for other modified gravity models (e.g. [47, 79].)

To follow the formation of structures within the ReBEL framework we used an adapted version of the GADGET2 code [80]. For the detailed descriptions of the modifications made to the code we refer the reader to our previous paper on this subject [28]. We conducted a series of high-resolutions DM only N -body simulations containing 512^3 particles within a periodic box of $32h^{-1}$ Mpc comoving side length. We used the canonical Λ CDM cosmology with $\Omega_m = 0.3$, $\Omega_\Lambda = 0.7$, $\sigma_8 = 0.8$ and $h = 0.7$. Our simulation had a $m_p \simeq 2.033 \times 10^7 h^{-1} M_\odot$ mass resolution and used a $\varepsilon = 6h^{-1}$ kpc force softening parameter. In this study we limit our analysis to the $z = 0$ epoch, leaving the time evolution of the ReBEL models as potential future work. Furthermore, the choice of a small simulation box size is motivated by our choice to have very high mass and force resolutions. This is done at the expense of a statistically relevant number of high-mass objects. However, in this work we want to emphasize the fifth-force effects induced on galaxy and dwarf sized DM haloes. Hence, we tailored our simulations for that purpose, leaving the high-mass and large-scale studies for future studies. The parameters of our simulations are summarised in Table 1.

Before going further, we would like to make some remarks concerning our numerical setup. When choosing such a high initial redshift for our simulations, we must be careful as this can be connected with additional unwanted effects. The problems are two-fold: (i) First, at such a high redshift the density fluctuations have very small amplitudes and therefore the N-body representation of the continuous density field is more prone to shot-noise effects related to the discrete nature of N-body particles. However, we checked that the initial as well as intermediate times power spectra against shot-noise effects and found that the density perturbations are represented faithfully down to the Nyquist limit ($k_{Nyq} \sim 50h/Mpc$) of our simulations. (ii) Secondly, as the GADGET2 code uses a finite-difference scheme for force interpolation, small particle accelerations at early times are prone to a larger relative error in force estimation. It can affect our results if the relative error is much larger for the ReBEL runs than in the Λ CDM case. To overcome this, we adapt a modified cell-opening criterion for the ReBEL runs, such that the relative error in the sum of the gravitational and fifth forces is consistent with the original (i.e. Newtonian) relative error of the acceleration. This modifications is similar to the setup developed by Keselman *et al.* [20], for a detailed discussion we refer the reader to the appendix of [20]. Moreover, we employ a fine mesh size ($l_{cell} = 31.25h^{-1}$ kpc) for the PM part of the gravitational force calculation of GADGET2 that is much smaller than the characteristic screening length $l_{cell} \ll r_s$. Thanks to this, the relative error in the estimation of the gravitational and fifth forces differs by an insignificant amount from the usual Newtonian error (see Eqn. A2 in [20]).

We used the MPI+OpenMP hybrid AMIGA halo finder (AHF), which is the successor of the MHF halo finder [81], to identify haloes and subhaloes in our simulation⁴. For a detailed description of AHF see the code paper [82]. We identify haloes using R_{200} as halo edge. This radius is defined,

⁴AHF is freely available from <http://popia.ft.uam.es/AMIGA>

as the distance at which the overdensity within a sphere centred at the halo centre satisfy:

$$\bar{\rho}(r_{200}) \sim 200 \cdot \rho_{crit}, \quad (3.1)$$

where ρ_{crit} is the critical density for a flat Universe. We take the R_{200} and M_{200} values as the virial radius and mass of a halo. It is important to note that we needed to adjust the code to take into account the fifth force of the ReBEL models. We have modified the unbinding procedure for removing the gravitationally unbounded particles by using the modified potential laws of the ReBEL model. Moreover we also changed the halo circular velocity equation. We need to take into account that DM particles, due to the additional scalar force, have higher potential energies in ReBEL compared to Λ CDM. The proper circular velocity equation at distance R_{200} in the ReBEL DM haloes has the following form:

$$\begin{aligned} V_c^{ReBEL} &= \left[\frac{GM_{200}}{R_{200}} \cdot \left(1 + \beta(1 + R_{200}/r_s)e^{-R_{200}/r_s} \right) \right]^{1/2} = \\ &= V_c \cdot (F_s(\beta, R_{200}/r_s))^{1/2}, \end{aligned} \quad (3.2)$$

where M_{200} is DM mass inside R_{200} , V_c is the circular velocity for pure Newtonian dynamics and F_s is the ReBEL force factor given in Eq. (2.22). This expression can be found by noting that on a circular orbit the centripetal force acting on a DM particle has an additional component coming from the scalar interactions.

Throughout this paper we limit our analysis, if not explicitly stated otherwise, to DM haloes that contain at least 100 DM particles. Thus we set our minimal halo mass to $M_{min} = 2.03 \times 10^9 h^{-1} M_\odot$.

3.1 The effects of baryons

The simulations used in this paper contain only a collisionless component. In other words, our approach treats baryons as part of dark matter component, since the only baryonic effects that we consider are those incorporated in the initial transfer function (the BAO wiggles). Obviously, such an approach is a severe simplification of the real universe since it is well known that hydrodynamical and gas effects play a crucial role in galaxy formation [83–85]. At the same time, the presence of a baryonic component affects the DM distribution, with crucial effects especially in the inner parts of haloes [86–88]. This interplay between baryons and DM is further complicated in the ReBEL scenario due to the breaking of the weak equivalence principle. As this effect by itself is very interesting and leads to a more complicated picture (see e.g. [89, 90]), we choose to focus only on the net effects induced by the fifth-force approximation on the DM distribution. We do so because the plethora of complicated baryonic feedback processes (including effects such as radiative cooling, reionisation, supernova and AGN feedbacks) would be very hard to disentangle from effects induced purely by the modified gravity. In fact, Puchwein *et al.* [91] showed that in some class of fifth force models, baryonic feedback processes can have opposite effects compared to the fifth force ones. Moreover, a proper modelling of galaxy-scale baryonic processes depends on a suitable choice and tuning of sub-grid physics parameters. Therefore, being fully aware of the limitation of our approach we decided to leave at a side the baryonic component for this current study.

4 Results: Statistical properties of the halo populations

In the subsequent analysis we focus on characterises how the presence of the long-range scalar interactions affect the whole population of DM haloes. In doing so we compare the differences between the fiducial Λ CDM cosmology and the ReBEL models on the basis of changes in the distribution and statistical means of halo properties like density profile, spin and halo shape.

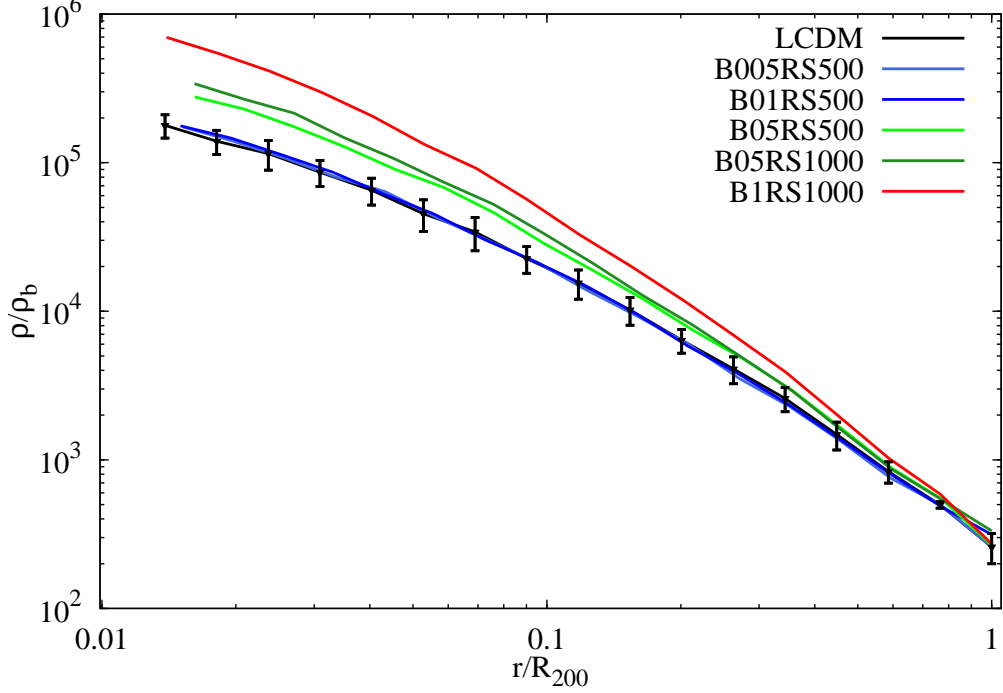


Figure 2. The spherically averaged density profiles for the 10 Most Massive Haloes of the Λ CDM and ReBEL runs.

4.1 Density profiles

Our phenomenological ReBEL models effectively change the strength of gravity on scales $r \leq r_s$, thus we expect to see changes in the internal structure of DM haloes. One way to quantify these changes is via the halo density profile. To get good statistics and eliminate the halo to halo variation, we compare the density profiles obtained from averaging over the 10 Most Massive Haloes (MMH10) found in each of our simulations. These haloes have masses in range $10^{13} M_\odot h^{-1} < M_{200} \lesssim 10^{14} M_\odot h^{-1}$. We focus only on the most massive haloes since they have virial radii larger than $\approx 400 h^{-1}$ kpc. In the B005RS500, B01RS500 and B05RS500 models the size of these massive haloes is comparable to the screening length of the fifth force, whereas for B05RS1000 and B1RS1000 the screening length is larger than the virial radii. Hence we suspect that any significant deviations in the density profiles due to the ReBEL model should be imprinted in these massive haloes. The averaged density profiles for all the runs are shown in Figure 2. We find that in the inner parts of the MMH10 ($r < 0.1 R_{200}$) the ReBEL haloes have higher density than the fiducial objects from the LCDM run. Thus we can expect that the counter-partners of the LCDM MMH10 have higher concentrations. To asses this and better understand the density differences between models we use the well known Navarro, Frenk & White (NFW) profile [92]. This was shown to be a universally good fit for the majority of Λ CDM haloes. The NFW profile is given as:

$$\rho_{NFW}(R) = \frac{\rho_0}{(R/R_s)(1 + R/R_s)^2}. \quad (4.1)$$

Here ρ_0 and R_s (not to be mistaken with r_s - the scalar force screening length parameter) are the parameters of the density profile fit. The first parameter is the characteristic density and the second one is the scaling radius. The scaling radius is usually used to define the concentration parameter c_{200}

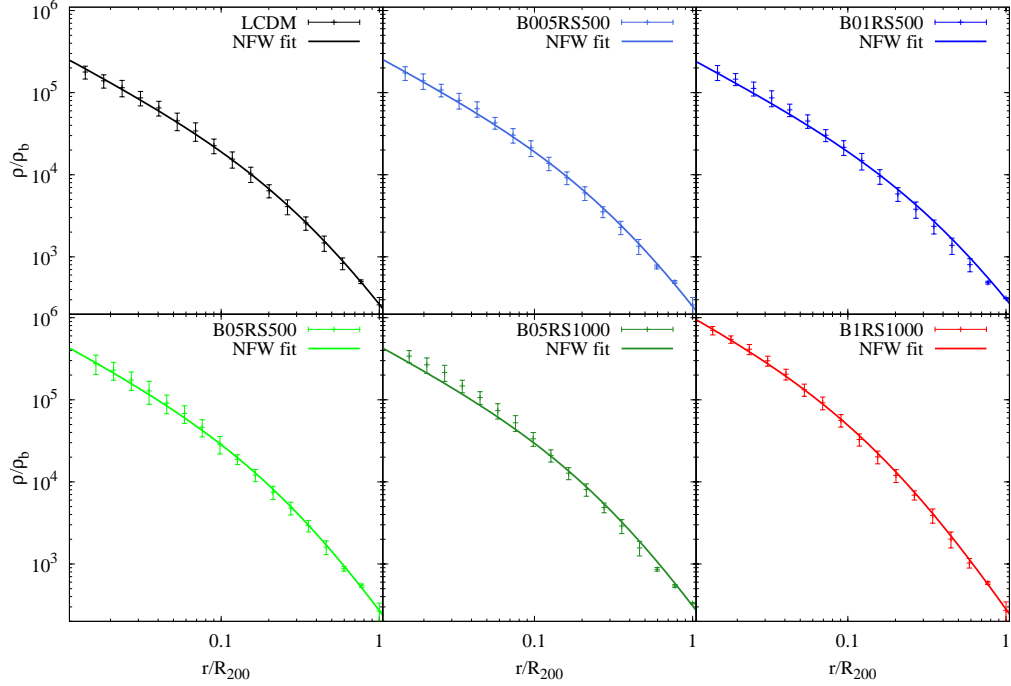


Figure 3. The MMH10 density profiles shown separately, together with the best NFW fits.

of a given *NFW* density profile:

$$R_{200} = c_{200} \cdot R_s, \quad (4.2)$$

where R_{200} is the virial radius of the halo.

The NFW fits to each of the MMH10 density profiles are shown in Figure 3. Each panel in the figure shows the profile and the fit for the 10 most massive haloes in that simulation run. We find that the NFW profile is a reasonably good fit for all our massive haloes, with small deviations only for some models below $0.1 R_{200}$. These deviations are not surprising since it is well established that the NFW profile is poorly describing very massive haloes that, in general, are not that well relaxed [93]. Thus we conclude the universality of CDM halo density profiles even in the presence of a fifth force with different screening lengths. The parameters of the NFW fits are summarised in Table 2. We find

Table 2. The NFW best fit parameters for MMH10 density profiles.

Model	ρ_0	R_s/R_{200}	c_{200}
LCDM	6624	0.4343	2.303
B005RS500	7133	0.4111	2.433
B01RS500	5499	0.4988	2.005
B05RS500	16772	0.3008	3.324
B05RS1000	15153	0.3299	3.031
B1RS1000	63885	0.1831	5.463

that the most massive haloes in the ReBEL runs are characterised by higher characteristic densities and smaller scaling radii which in turn mean higher virial concentrations. We confirm such findings for all ReBEL MMH10s except the B01RS500 case. For this model the best NFW fit is characterised actually by lower concentration than the LCDM case.

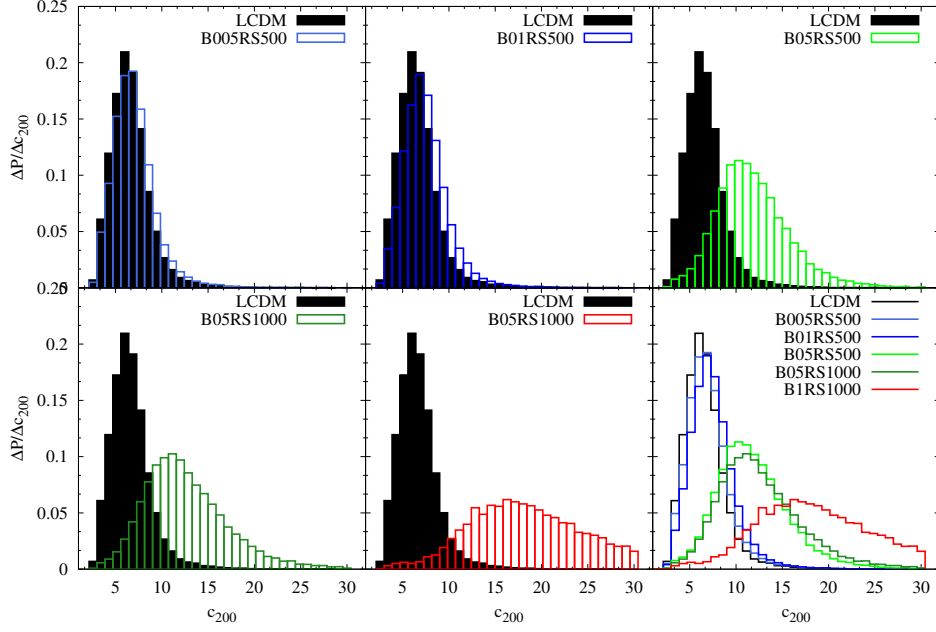


Figure 4. The distributions of the virial concentration parameter for all haloes in our ReBEL models. Each panel shows also the fiducial Λ CDM case for comparison.

We find that the NFW fit is universally good in describing the density profile for the majority of haloes in the ReBEL runs, not only for the most massive ones. Fitting the density profile with a NFW function results in a concentration parameter c_{200} for each halo. This c_{200} parameter is a measure of the imprint of the fifth force onto the haloes inner structure. The distribution of the concentration parameter for each run, for all the haloes, is shown in Figure 4. In each panel, on top of the respective ReBEL run, we plot with black boxes the distribution obtained from the LCDM run which is the fiducial case to compare with. The bottom-right panel presents distributions for all runs to allow for a direct comparison between ReBEL models. We find that the ReBEL haloes are characterised by broader distributions with higher values of the mean c_{200} parameter. These findings are summarized in Table 3.

Table 3. The mean and standard deviation of the c_{200} distributions when fitting NFW profiles to the whole halo population.

Model	$\overline{c_{200}}$	$\sigma_{c_{200}}$
LCDM	5.9	2.7
B005RS500	6.3	2.7
B01RS500	6.81	2.8
B05RS500	11.32	4.2
B05RS1000	12.15	4.9
B1RS1000	19.24	8.0

Thus, on average, the ReBEL haloes have higher concentrations. This effect is small only when we consider more realistic models with small β value. For B005RS500 the mean concentration is only 6.7% higher then in the LCDM case. For the B01RS500 model, the deviation reaches already 15.4%. When we look at the remaining models with $\beta \geq 0.5$ the effects become dramatic with the increase of

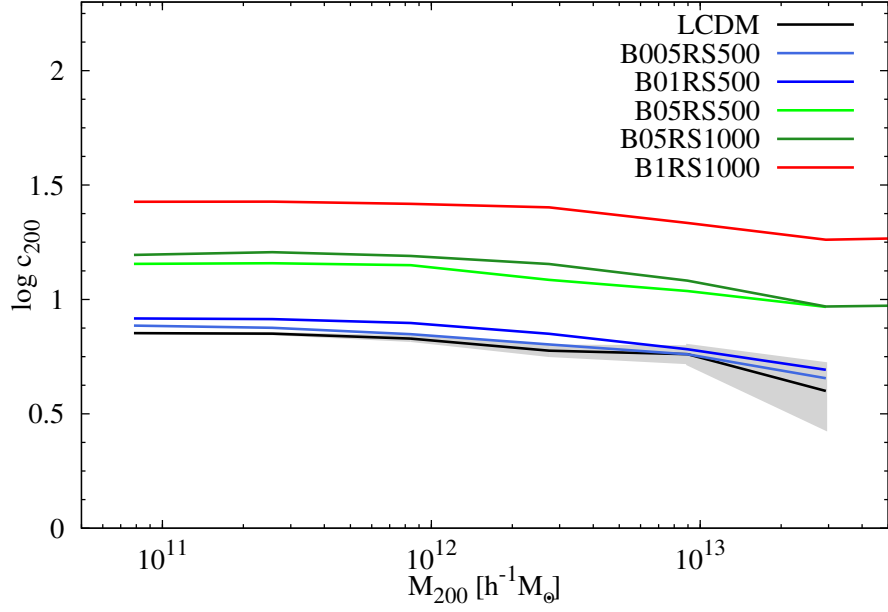


Figure 5. The mass-concentration relation. The median c_{200} binned in halo mass is plotted for all models. The shaded region marks the bootstrap error of the median for the Λ CDM case.

the mean concentration $\overline{c_{200}}$ from 92% for B05RS500 all the way to 300% for B1RS1000. The mean concentration for strong fifth force models shows a significant difference from the standard model, with values that are 2 to 5σ higher than the Λ CDM mean. However the distributions plotted in Figure 4 are dominated by low mass objects, which biases our result to small haloes. We investigate how these findings change as a function of halo mass in Figure 5. The plot gives the median c_{200} binned in halo mass for our models. The figure also shows the 1σ bootstrap error in the determination of the median for Λ CDM which quantifies how significant is the deviation given our limited halo sample. It is clearly seen that the median concentration is systematically shifted towards higher values for all ReBEL models and for all halo masses.

This can potentially mean bad news for the ReBEL cosmology. Such a noticeable increase of the mean concentration poses additional challenges to the problem of the bright dwarf satellites of the Milky Way galaxy [94–96]. But we must admit that the full self-consistent quantification of this problem requires simulations in a bigger box (to obtain a larger sample of Milky Way-like objects) that additionally must also contain a baryon component with full hydrodynamical solution. Ergo we will not discuss this problem any more in this work.

Higher concentrations of the ReBEL haloes are the outcome of boosted hierarchical structure formation in this class of models. This induces earlier formation times for the majority of haloes as reported by Hellwing et al.[30], which potentially can be desired to solve some of the challenges of Λ CDM (see the introduction for a discussion of such problems). But this is a double-edged sword that comes at the price of raised halo concentrations which poses additional difficulties.

4.2 Spin & halo rotation

According to the tidal torque theory the angular momentum of a galaxy/DM halo is growing thanks to the gravitational tidal interactions between the DM proto-halo and the matter distribution surrounding

it [97–102]. Thus we can express the angular momentum gained by the halo as

$$\mathbf{J}_i \propto \varepsilon_{ijk} \mathbf{I}_{jl} \mathbf{T}_{lk}, \quad (4.3)$$

where \mathbf{I}_{jl} is the inertia tensor of the proto-halo and \mathbf{T}_{lk} is tidal torque tensor generated by the matter distribution in the vicinity of the halo. These tidal torque forces are also shaping the characteristic web-like pattern of the matter distribution on large-scale, hence providing a connection between the angular momenta of DM haloes and the matter distribution on Megaparsec scales. However, the late-time dynamical evolution imprints non-linear and gasodynamical effects that strongly erase primordial connection between the matter distributions and angular momenta of DM haloes. In hierarchical structure formation scenarios the highly non-linear processes like tidal stripping, close encounters and major mergers dominate the growth of the angular momentum at intermediate and small redshifts (see details in e.g. [103–107]). Nevertheless, knowing that in ReBEL cosmologies the attractive forces shaping the evolution of DM are enhanced on Megaparsec scales, we expect to see imprints of the scalar fields in the angular momentum of haloes.

The spin parameter

The angular momentum of a DM halo is commonly parametrised by the dimensionless spin parameter [98]

$$\lambda = \frac{|J||E|^{1/2}}{GM^{5/2}}, \quad (4.4)$$

where E is the total mechanical energy of the halo, M is its mass, G is Newton’s gravitational constant and J is the total angular momentum. There is another common definition of the dimensionless spin parameter proposed by Bullock *et al.* [108]. This second definition is more convenient to implement computationally and we decided to use it in our study. The Bullock spin parameter is defined as

$$\lambda = \frac{|j|}{\sqrt{2}R_{200}V_c}, \quad (4.5)$$

where

$$V_c = \left(\frac{GM_{200}}{R_{200}} \right)^{1/2} \quad (4.6)$$

is the circular orbit velocity at R_{200} and j is the specific angular momentum of the halo

$$j = \frac{1}{N_H} \sum_{i=0}^{N_H} r_i \times v_i. \quad (4.7)$$

Here the sum covers all particles belonging to a given DM halo $0 \leq i < N_H$. Equation (4.6) is correct for Newtonian gravity, but for ReBEL haloes we have to use the modified circular orbit velocity given by Eq. (3.2). The spin parameter as defined above measures the rotational support of a halo. High values of λ corresponds to haloes that are spinning fast, while a low λ indicates a slowly rotating halo.

Our halo catalogues are dominated by low-mass objects with $M_{200} \leq 2 \times 10^{10} M_\odot/h$. We have checked that for these dwarf-like objects the differences in spin parameter distributions between Λ CDM and ReBEL are very small. The strongest difference was noted for the B05RS500 model, but that accounted to less than $\approx 5.2\%$ of the mean Λ CDM spin parameter. Therefore in the following analysis we focus on bigger galaxy-like haloes with $M_{200} > 10^{11} M_\odot/h$. For this population of objects the deviations from the fiducial model are more prominent.

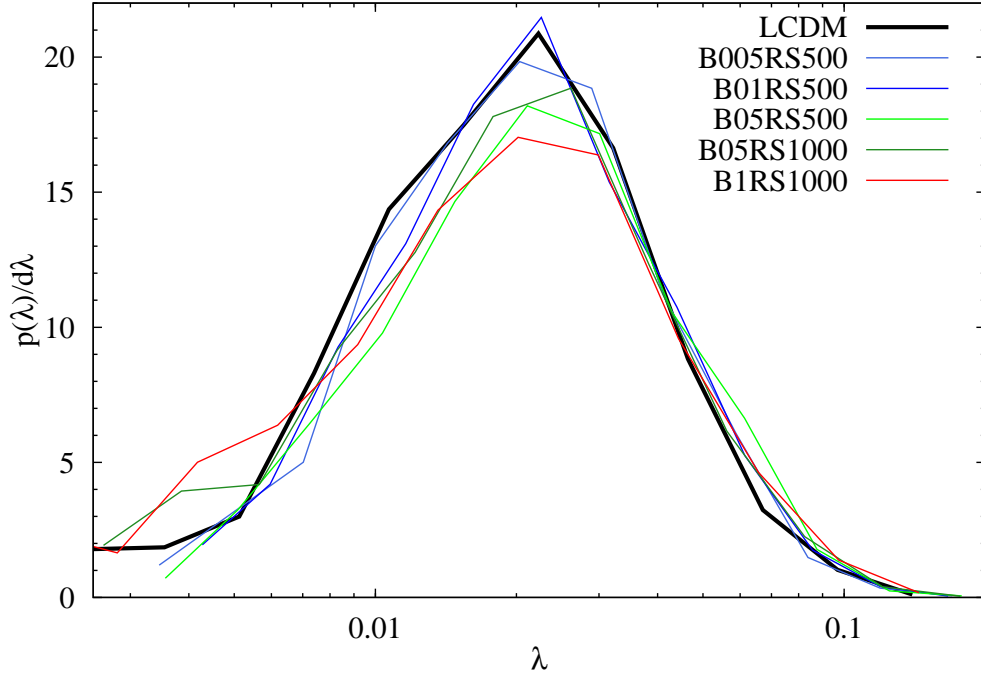


Figure 6. Distributions of the spin parameter λ for our models.

Figure 6 gives the spin parameter distributions for our six simulations. We observe that there are clear differences between the Λ CDM and ReBEL spin distributions. The fifth force models have a broadening and flattening of the distribution, with more prominent high and low spin tails. There also seem to be a shift of the distribution centre towards higher λ values when compared to the Λ CDM case. Therefore we conclude that haloes in the ReBEL cosmologies have, in a statistical sense, higher spin values, thus are spinning faster than Λ CDM haloes. We note that the largest deviations from Λ CDM appear for the strongest ReBEL models studied in this work, i.e. for B05RS1000 and B1RS1000. The shift of the spin distribution centres – however noticeable – does not appear to be large. To check the statistical significance of this effect we use that the spin parameter distribution in N-body simulations is well approximated by a log-normal function given by

$$p(\lambda)d\lambda = \frac{1}{\lambda\sigma\sqrt{2\pi}} \exp\left[-\frac{(\ln\lambda - \mu)^2}{2\sigma^2}\right] d\lambda, \quad (4.8)$$

with the centre of the distribution in the range $0.04 < \lambda < 0.05$ [109–113]. The log-normal distribution has the mean value (i.e. first moment) given by

$$\lambda_0 = e^{\mu + \frac{1}{2}\sigma^2}, \quad (4.9)$$

and the standard deviation as

$$\sigma_\lambda = e^{\mu + \frac{1}{2}\sigma^2} \sqrt{e^{\sigma^2} - 1}. \quad (4.10)$$

In Figure 7 we plot the distributions of the λ parameter and their corresponding best-fit log-normal functions as given by Eq. (4.8). Each panel shows the spin distribution and log-normal fit for that given model. The best fit log-normal functions describe reasonably well the underlying distributions for all models – even for the strongest ReBEL run. The parameters of these fits are presented

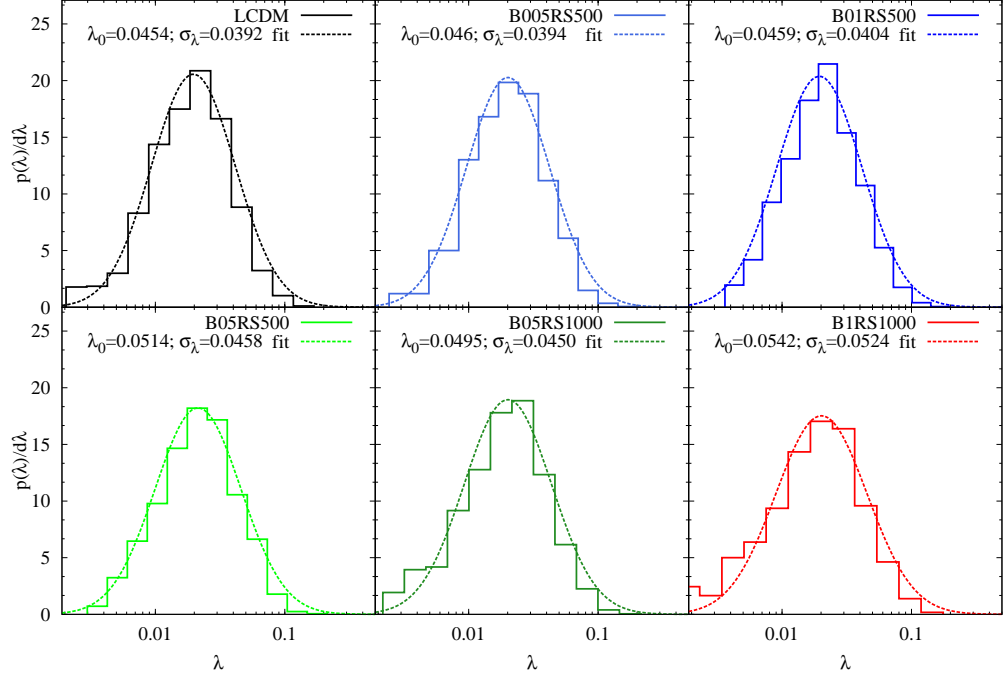


Figure 7. The distributions of the spin parameter accompanied by the fitted log-normal distributions. In each panel we also give the numerically computed mean value and the standard deviation of the shown distribution.

Table 4. The mean and standard deviation for the best log-normal fit to the spin distributions.

Model	λ_0	σ_λ
ΛCDM	0.0454	0.0392
B005RS500	0.0460	0.0394
B01RS500	0.0459	0.0404
B05RS500	0.0514	0.0458
B05RS1000	0.0495	0.0450
B1RS1000	0.0542	0.0524

in Table 4. The mean λ_0 and standard deviation σ_λ of the log-normal fit are gradually increasing as we move from Λ CDM to the strongest ReBEL model B1RS1000, in complete agreement with the qualitative observations we made for Figure 7. The maximum change in λ_0 appears between the Λ CDM model and B1RS1000 and amounts to over 19%. Although this increase in λ_0 is not large, it is accompanied by the more dramatic broadening of the distributions. The increase in σ_λ due to the presence of the scalar forces reaches nearly 33% when comparing Λ CDM and B1RS1000. Therefore, on average, there are more fast rotating haloes in ReBEL than in the standard Λ CDM cosmology. This can be a potentially positive effect, as fast rotating DM haloes promote easier thin-disk spiral galaxy assembly [114, 115].

Earlier studies of the halo spin in Λ CDM N-body simulations found that there is a weak dependence of λ on halo mass [116–118]. The observed dependence shows that more massive haloes tend to have slightly lower spin parameters. The spin-mass dependence for Λ CDM and ReBEL is shown in Figure 8 where we plot the median spin parameter as a function of the halo mass. The error bars, plotted only for the Λ CDM case, represent the first and the last quadrille over the median. For

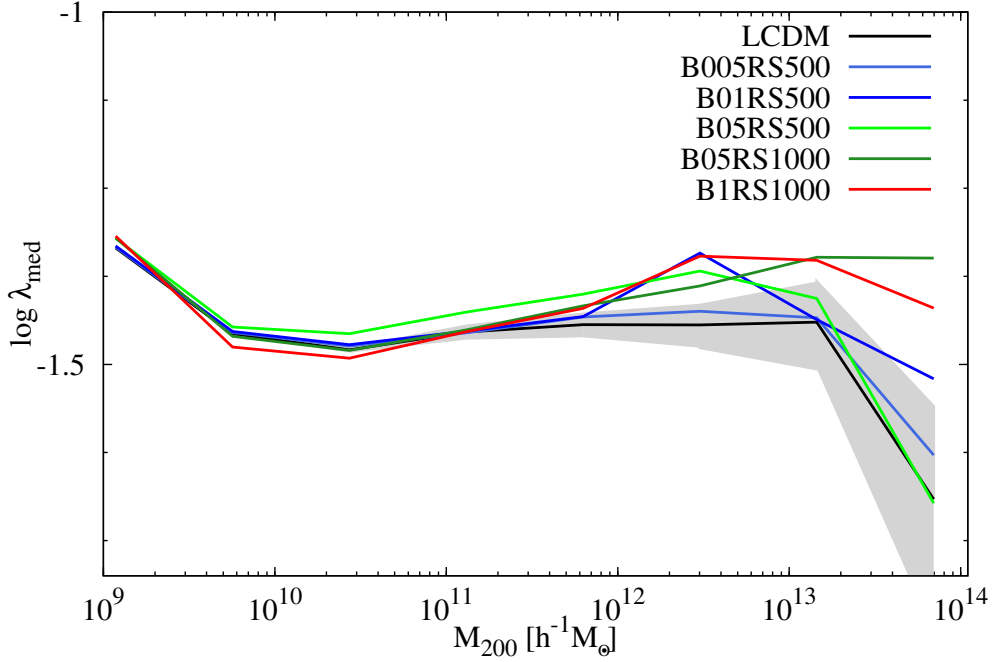


Figure 8. The $\lambda - M_{200}$ correlation for all our models. The shaded region reflects the error in the determination of the median λ . For clarity the errors are plotted only for the Λ CDM case.

Λ CDM we observe that there is a marginal dependence on mass of the form $\lambda \propto M^\alpha$ with the mean slope $\alpha = -0.005$. This is in agreement with other halo spin studies [116, 118]. When it comes to the ReBEL results, we find deviations from the fiducial Λ CDM behaviour. The average spin of low-mass haloes is affected only very weakly by the modified DM gravity. On the other hand, for massive objects we observe a strong increase of the mean spin compared to the Λ CDM case. The presence of a fifth force breaks the weak spin-mass dependence because it affects more strongly the massive haloes which tend to spin faster than the low mass one. Our simulations are not suited to quantify the spin-mass relation for ReBEL since we have only few objects at masses $M \geq 10^{12} M_\odot/h$ that give most of the variation with mass. A detailed analysis of the ReBEL effects on the spin-mass relation and the spin of cluster-like haloes needs a much better sample of massive objects that can be obtained only in simulations with a larger volume. Hence we leave this subject for a future study.

It is interesting to note that for all ReBEL models – except the runs with $r_s = 1000 h^{-1} \text{ kpc}$ – the λ_{med} values approach the Λ CDM limit for $M_{200} > 10^{13} h^{-1} M_\odot$. Using that the mass of a halo corresponds to some length scale that is related to the virial radius R_{200} , the above result implies that the halo spin for objects with large R_{200}/r_s ratios is less sensitive to the presence of a fifth force. These observations agree with the tidal torque theory of halo’s angular momentum and spin. The scale of the tidal forces shaping the halo spin is related to a halo’s virial radius. Thus for big haloes the enhancement of forces on scales smaller than it’s radius do not contribute significantly to the growth of its angular momentum.

4.3 Shapes and geometry

The shape and the geometry of a halo are determined jointly by linear and non-linear processes. Theoretical predictions are usually constrained to the linear processes influencing the shape of a DM halo. The high complexity characterising the non-linear phenomena acting within a halo makes

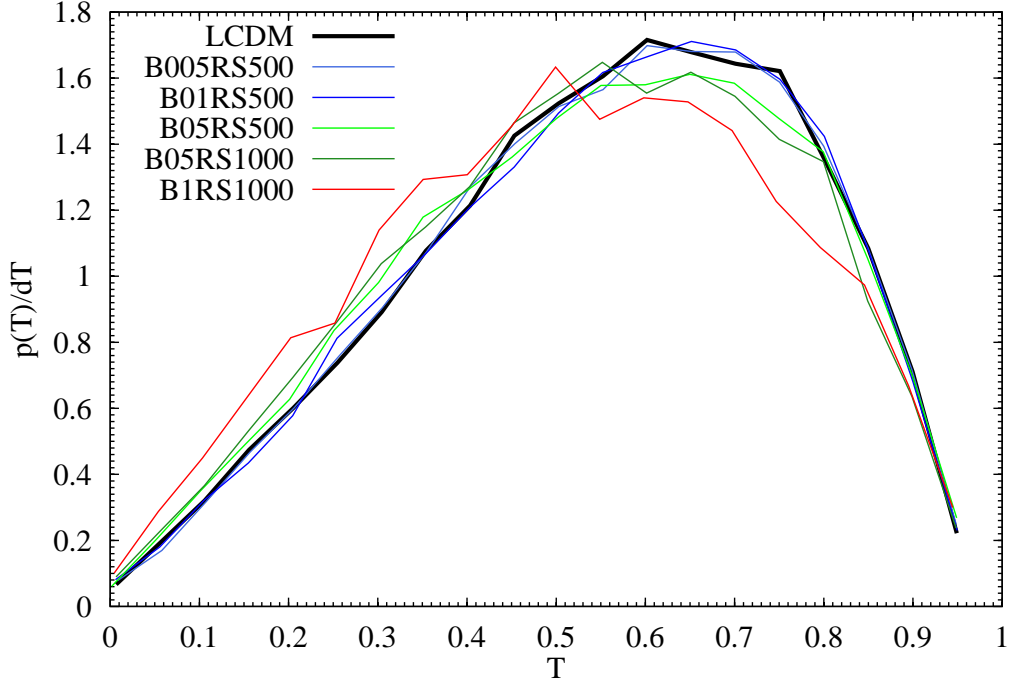


Figure 9. The distribution of the halo triaxiality parameter T in our six models.

predicting the direct outcome of such processes very difficult. Generally one assumes that three principal factors are responsible for the shape of an halo:

- the shape and orientation of the primordial density peak from which the halo originated [119–122],
- the external tidal shear field that shapes the halo [123, 124],
- and the non-linear interactions disturbing the original halo shape, e.g. the violent relaxation and halo merging [125].

The complex interplay of the above factors determines the final halo shape and geometry. In the following we check to what extent the presence of additional DM scalar-interactions affects the shape of the DM halo.

We determine the halo shape approximating its mass distribution to a triaxial ellipsoid. The halo’s axes of inertia are calculated from the moment of inertia tensor, which we define as:

$$I_{ij} = \sum_n^{N_H} x_i x_j, \quad (4.11)$$

where the particle positions x_i and x_j are with respect to the centre of mass of the halo and the sum covers all particles that belong to that given halo identified by the AHF. The axes of the ellipsoid are found using the eigenvalues λ_i of the inertia tensor via:

$$\begin{aligned} a &= \sqrt{\lambda_1}, \\ b &= \sqrt{\lambda_2}, \\ c &= \sqrt{\lambda_3}, \end{aligned} \quad (4.12)$$

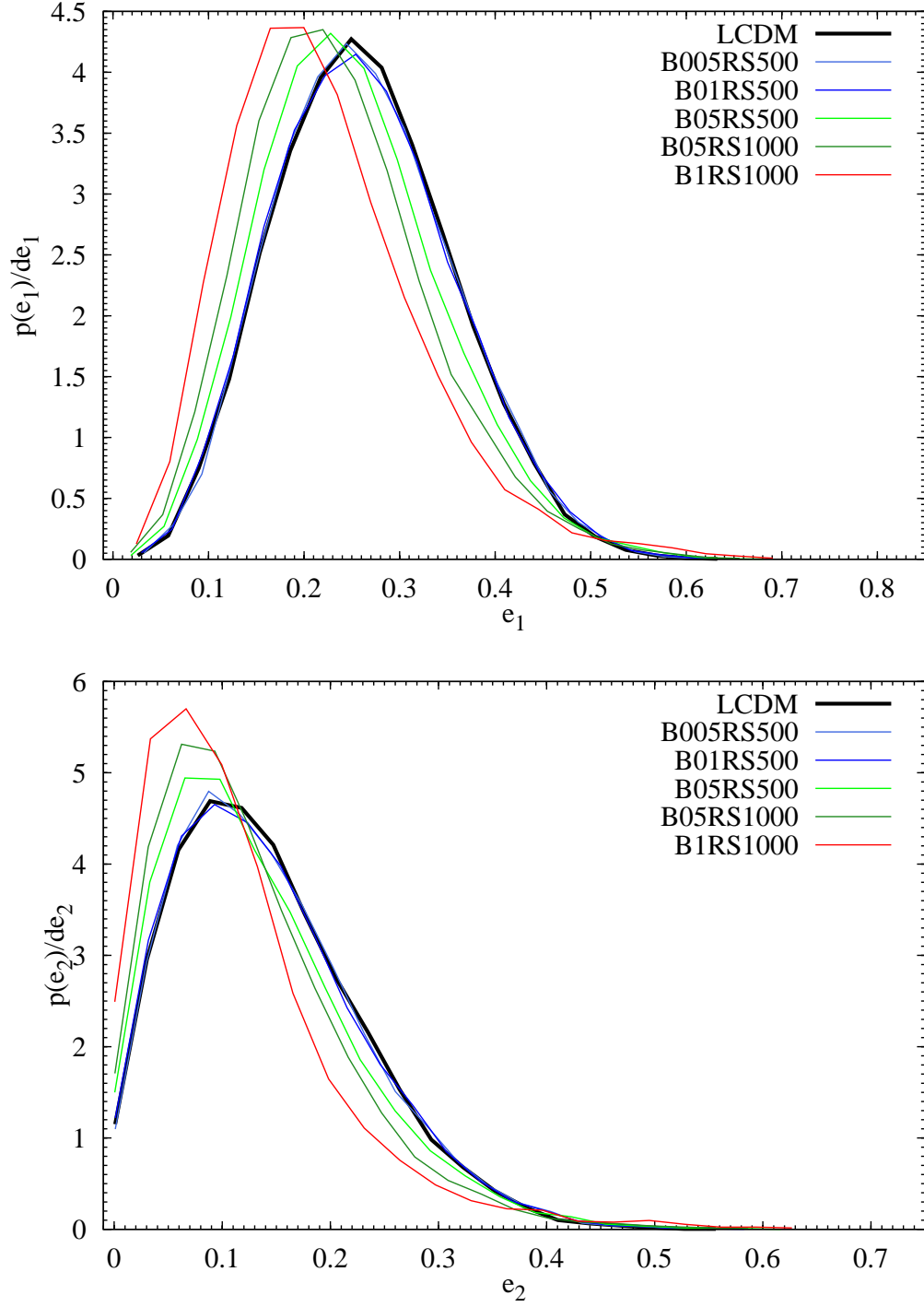


Figure 10. The distribution of the halo ellipticity parameter e_1 (top panel) and e_2 (bottom panel) in our six models.

with $a > b > c$. As our main measure of the halo shape we use the triaxiality parameter [126]:

$$T = \frac{a^2 - b^2}{a^2 - c^2}. \quad (4.13)$$

High values of T mark a prolate ellipsoid, while low values correspond to an oblate halo. There are two additional parameters related to the triaxiality, namely the ellipticity parameters e_1 and e_2 , which are defined as:

$$e_1 = 1 - \frac{c}{a} \quad \text{and} \quad e_2 = 1 - \frac{b}{a}. \quad (4.14)$$

The higher the values of these parameters the less spherical is the ellipsoid's projection in the planes of the related semi-axis.

Table 5. The mean and the standard deviations of the shape parameter distributions for all our models.

Model	$\langle T \rangle$	σ_T	$\langle e_1 \rangle$	σ_{e_1}	$\langle e_2 \rangle$	σ_{e_2}
Λ CDM	0.581	0.211	0.279	0.091	0.156	0.086
B005RS500	0.582	0.211	0.279	0.092	0.156	0.087
B01RS500	0.582	0.212	0.279	0.093	0.157	0.088
B05RS500	0.572	0.216	0.266	0.093	0.148	0.089
B05RS1000	0.564	0.215	0.253	0.094	0.139	0.086
B1RS1000	0.547	0.221	0.239	0.100	0.129	0.091

The distributions of the shape parameters T , e_1 and e_2 for our whole halo population is shown in Figures 9 and 10. These figures illustrate that: (i) haloes for models B005RS500 and B01RS500 have distributions of the shape parameters in very good agreement with the Λ CDM case; (ii) on the other hand remaining ReBEL models with a much higher β parameter show significant departures from the control sample; (iii) measured differences are stronger for the ellipticity parameters rather than for the triaxiality. The distributions of the ReBEL shape parameters are shifted towards values indicating more spherical shapes.

To outline this claim, we collected in Table 5 the mean values of the shape parameters alongside the distribution scatter σ for all six runs. The values in the table highlight that indeed the distributions of the shape parameters for models Λ CDM, B005RS500 and B01RS500 are nearly indistinguishable. The haloes in the models with stronger scalar forces have shapes noticeably different. For the strongest model - B1RS1000 - we find mean T lower by 6%, e_1 lower by 15% and e_2 by 18% compared to the Λ CDM case. This effect can have pronounced consequence for clusters and the conundrum of the degree of anisotropy of their velocity dispersions. Due to the limited volume of the simulation we cannot quantify properly the shape changes for clusters. Nonetheless the more spherical shapes of ReBEL haloes could indicate that on averaged they are better virialised. This can be due to the gravity enhancing effect of the scalar interactions that, in turn, promote earlier structure formation and faster dynamical relaxation.

4.4 Virialisation

To investigate the virialisation state of our haloes we use the the Virial Theorem. A halo is virialised when:

$$2K + U = 0. \quad (4.15)$$

However the above assumes that a halo is in complete isolation and that all the mass connected to the halo has been taken into account. The AHF code we use to identify haloes makes a cut at the outer boundary which corresponds to the radius at which the spherically averaged density is $\Delta_{200} = 200 \times \rho_{crit}$. Particles bound to the halo, but outside this boundary, are not used to compute the overall kinetic and potential energies. However these particles do affect the virial state of the halo

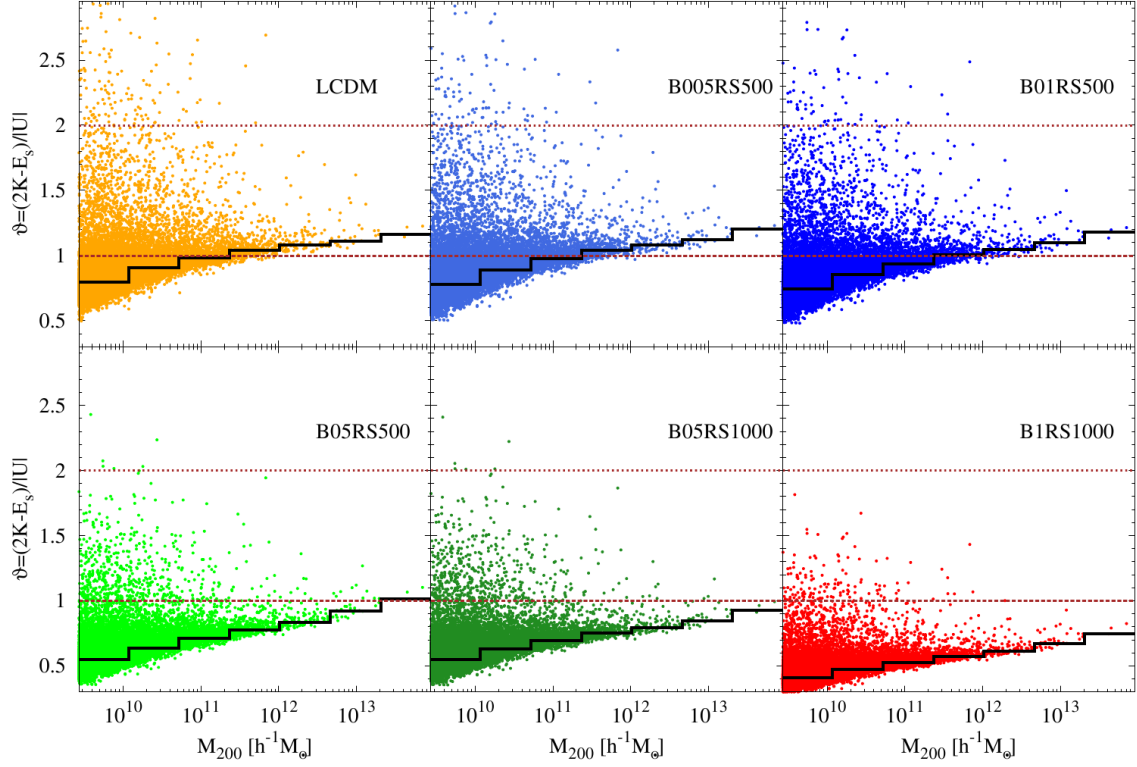


Figure 11. The virial ratios for haloes in all models. Panels show results from the Λ CDM (top-left) to B1RS1000 (bottom-right). In each panel the points show results for individual haloes while the solid black lines depict the median values computed in each mass bin. Horizontal lines mark the virialisation threshold $\mathcal{V} = 1$ (the dashed line) and the gravitational bound threshold $\mathcal{V} = 2$ (the dotted line).

and can be accounted for in the form of the pressure term E_s . We compute this term for each halo individually using the method described in [127].

Using Eq. (4.15) we define the virial ratio parameter (now including the pressure term) \mathcal{V} , which is a measure of the virial state of an object (for a more detailed and elaborate discussion about a halo’s virial state see e.g. [128]):

$$\mathcal{V} = \frac{2K - E_s}{|U|}. \quad (4.16)$$

The virial ratio approaches unity for a fully virialised halo, it is in range $1 < \mathcal{V} \leq 2$ for gravitationally bound system while $\mathcal{V} > 2$ depicts an unbound object.

The ReBEL gravitational potential (see Eq. (2.18)) suggest that halos with $R_{200} \ll r_s$ have a gravitational bounding energy larger by factor of $1 + \beta$, effectively lowering the virialisation factor. However the forces that particles exert on each other are also increased providing to some extent higher accelerations, thus also higher velocity dispersions. These two effects have opposite contributions to the virialisation parameter \mathcal{V} . Nevertheless we can expect that on average haloes are more virialised in the ReBEL case.

The virial ratios for both Λ CDM and ReBEL models are presented in Figures 11 and 12. The former gives in the six panels the virial ratio as defined by Eq. (4.16) as a function of halo mass for each of our simulation runs. Dots represent the \mathcal{V} values for individual haloes while the solid black lines depict median virial ratio binned in halo mass. Each panel shows two brown horizontal

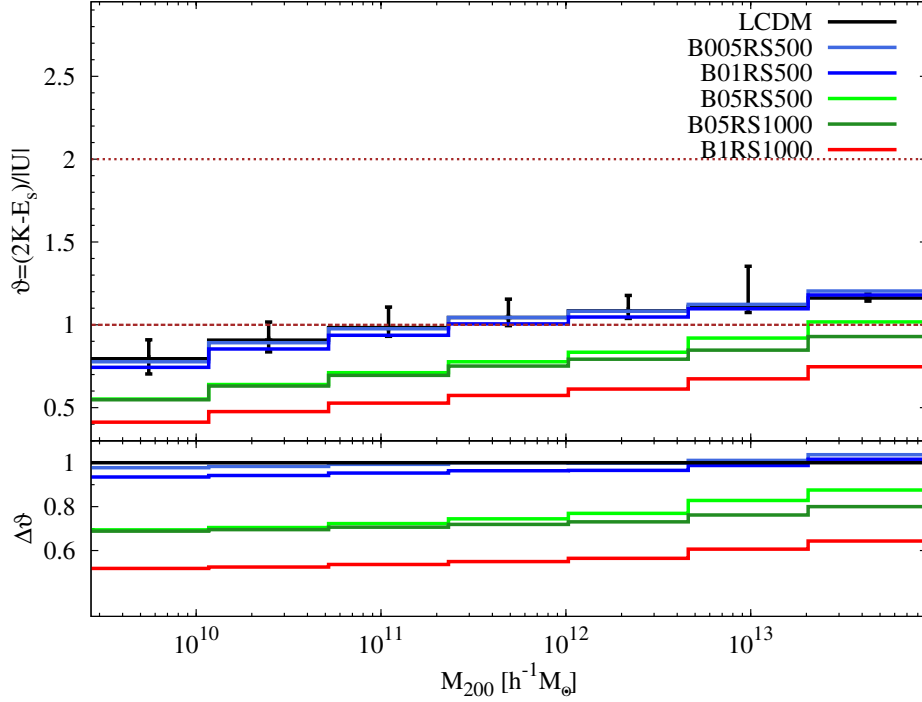


Figure 12. Top panel: the median virial ratios for all models binned in halo mass. The error bars represent the upper and lower quartiles of the sample and are plotted only for the Λ CDM case. Bottom panel: The deviation $\Delta \mathcal{V} = \mathcal{V}_{\text{ReBEL}}/\mathcal{V}_{\text{LCDM}}$ of ReBEL virial ratios $\mathcal{V}_{\text{ReBEL}}$ from the Λ CDM case $\mathcal{V}_{\text{LCDM}}$.

lines marking the two virial ratio thresholds: a virialised state (the dashed line) and a gravitationally bounded state (the dotted line). The results presented in the figure clearly underline known effects, that on average smaller mass haloes tend to be closer to relaxation while massive ones ($M_H \gtrsim 10^{13} - 10^{14} h^{-1} M_{\odot}$) are less virialised systems. We immediately notice that in all our ReBEL runs the majority of DM haloes have lower values of the virial state \mathcal{V} than haloes in the fiducial Λ CDM run. This is clearly visible when looking at the lines depicting the averaged virial ratios binned in halo mass.

To study this effect in more detail we show in the top panel of Figure 12 the median values for the virial ratios. In the bottom panel of the same figure we plot the relative deviations of this quantity compared to the Λ CDM case $\Delta \mathcal{V} = \mathcal{V}_{\text{ReBEL}}/\mathcal{V}_{\text{LCDM}}$. Undoubtedly the ReBEL haloes, on average, are more virialised than their Λ CDM cousins. For models with $\beta \geq 0.5$ the effect is very prominent and amounts to 30% – 50% lower virial ratios. For the other two weaker fifth force models we find that the overall virial ratio is very close to the Λ CDM case, although systematically shifted towards lower values. Figure 12 also illustrates how the screening length affects the virial state of a halo. This can be seen when comparing the B05RS500 and B05RS1000 runs which have the same strength of the scalar forces $\beta = 0.5$, but differ in the screening length with $r_s = 500 h^{-1} \text{ kpc}$ and respectively $r_s = 1000 h^{-1} \text{ kpc}$. While these two models have the same median virial ratio for objects with $M \lesssim 2 \times 10^{11} h^{-1} M_{\odot}$, the run with a larger r_s has the massive haloes in a more virialised state.

5 Conclusions

This work studied the differences between Λ CDM and a specific implementation of exotic physics, the ReBEL model. The new physics considered here involves long-range fifth-forces between DM

particles that phenomenologically act as modified gravity. These forces are restricted to scales below $1h^{-1}\text{Mpc}$ due to the screening of the scalar field mediating this interaction. The ReBEL model is characterized by two free parameters: the ratio of the scalar to the gravitational force β and the screening length r_s . In this work we analysed five such models with different values of these two parameters to explore a range of allowed ReBEL cosmologies.

To assess the effects of the fifth force we conducted a series of high resolution N-body simulations that followed the formation and evolution of structure in both the ΛCDM and ReBEL models. Using the results of these simulations, we have focused our attention on understanding and quantifying how halo internal properties change as a function of the strength of the scalar interaction. We summarise our findings as follows:

- The density profiles of ReBEL haloes are well described by the NFW profile [92], but with higher concentrations. The increase in concentration ranges from a few percent for the weakest of our fifth-force model up to 300% (5σ away from the ΛCDM mean) for the case with the strongest scalar interaction. This result puts the high β ReBEL models at odds with current astronomical observations which favour smaller halo concentrations (e.g. see [129–137]). However, we must stress out that on this scales there are additional baryonic physics effects, which we did not include, that can change the picture significantly. Therefore, we need additional simulations with baryons in order to make a more realistic comparison between ReBEL predictions for the halo concentration and current observational data.
- The analysis of the halo spins distributions revealed that ReBEL haloes with $M_{200} \geq 10^{11} h^{-1} M_\odot$ are characterised by a higher mean spin λ_0 and standard deviations values. This indicates that DM haloes in fifth force models have higher rotational support and thus they spin faster. On the other hand, we did not find any significant boost to the spin of the low-mass haloes. The spin-acquiring mechanism is enhanced by ReBEL forces only in the regime of galaxy and cluster like haloes. This leads to the breaking of the ΛCDM weak spin-mass dependence, as the high mass haloes spin faster in ReBEL. The variation of the mean spin with mass is especially significant for the strongest scalar interaction models that we tested - B05RS100 and B1RS1000.
- Our studies showed that halo shapes are sensitive to the presence of a fifth force. For strong ReBEL models we found strong deviations of the triaxiality and especially ellipticity parameters from ΛCDM . Haloes in these models tend to be more spherical, which is a direct outcome of the fact that smaller mass haloes ($M_{200} \leq 5 \times 10^{11} h^{-1} M_\odot$) are more virialised in ReBEL than in ΛCDM . For weak scalar interacting models, $\beta \leq 0.1$, we find that the halo shape parameters are insensitive to the presence of this additional force.
- The comparison of the halo virialisation state in ΛCDM versus ReBEL showed that the scalar forces, in average, help haloes attain dynamical relaxation. This effect is only prominent for strong fifth forces. The models with $\beta \leq 0.1$ showed only a minor virialisation increase and only for objects considerably smaller than the screening length $r_s = 500h^{-1} \text{kpc}$.

Our findings give an interesting picture for ReBEL and similar fifth-force cosmologies. For the models in which the fifth force is small compared to gravity, we found that the differences in the measured halo properties are small. As we increase the strength of the fifth force, most of the halo properties, both as distributions and as mean values, start to deviate significantly from the ΛCDM case. But the clear and prominent signature of the scalar force in the DM haloes properties is obtained only for unrealistic values of the β parameter. Such strong scalar forces are incompatible with the observed

universe due to noticeably higher power spectrum and two-point correlation function. Moreover, we underline that the enhanced structure formation produces haloes with higher concentration parameters. This affects especially the dwarf halo regime ($M_{200} < 10^{10} h^{-1} M_{\odot}$) which puts ReBEL in conflict with the observations of the Local Universe, which are already a problem for Λ CDM [94–96]. However, we must stress that the severe effects seen in the profiles of small-mass ReBEL haloes do not necessarily trouble other modified gravity models (e.g. [34, 35, 40, 138–140]). Therefore, these effects may be a specific feature of the ReBEL cosmology where the fifth force is allowed to act starting with very early times of cosmic evolution.

Our results suggest that ReBEL cosmologies with large values of the β parameter make predictions that are at odds with current observational data, more so than the standard Λ CDM picture. The models with weak scalar interactions make similar prediction to the standard scenario and therefore it may be difficult to distinguish between the two. The general trend of changes induced by the ReBEL interactions shows that this class of modified gravity models provides at most a poor fix to the galaxy-scale challenges of the Λ CDM universe. Thus, we conclude that, in the light of this research, the ReBEL cosmology is no longer an interesting and appealing modification of the Λ CDM paradigm as it used to be.

Acknowledgments

Shortly after completing the first version of this paper our co-author and friend - Roman Juszkiewicz - had passed away. Filled with grief and muse we dedicate this work to his living memory. As we are grateful for Roman’s many ideas and encouragements. We would also like to thank the anonymous referee, whose comments and suggestions helped us significantly improve the scientific quality of this paper. The simulations used in this research were performed on the `Boreasz` supercomputer at the Interdisciplinary Center for Mathematical and computational Modelling of the University of Warsaw. This research was carried out with the support of the ”HPC Infrastructure for Grand Challenges of Science and Engineering” Project, co-financed by the European Regional Development Fund under the Innovative Economy Operational Programme. WAH would like to acknowledge the hospitality of the Institute of Astronomy at the University of Zielona Góra that he has received during his stay there. WAH also acknowledge the support of this resreach received from Polish National Science Center in grant no. DEC-2011/01/D/ST9/01960. AK acknowledges support by the Spanish Ministerio de Ciencia e Innovacion (MICINN) in Spain through the Ramon y Cajal programme as well as the grants AYA 2009-13875-C03-02, AYA2009-12792-C03- 03, CSD2009-00064, CAM S2009/ESP-1496 and partial support from the European Union FP7 ITN INVISIBLES (Marie Curie Actions, PITN-GA-2011-289442). He also thanks Burt Bacharach foralfie SRK acknowledges support by the Ministerio de Ciencia e Innovacion (MICINN) under the Consolider-Ingenio, SyeC project CSD-2007-00050.

References

- [1] E. Komatsu and et al., *Seven-Year Wilkinson Microwave Anisotropy Probe (WMAP) Observations: Cosmological Interpretation*, ArXiv e-prints (Jan., 2010) [[arXiv:1001.4538](https://arxiv.org/abs/1001.4538)].
- [2] M. Tegmark, M. A. Strauss, M. R. Blanton, K. Abazajian, S. Dodelson, H. Sandvik, X. Wang, D. H. Weinberg, I. Zehavi, N. A. Bahcall, F. Hoyle, D. Schlegel, R. Scoccimarro, M. S. Vogeley, A. Berlind, T. Budavari, A. Connolly, D. J. Eisenstein, D. Finkbeiner, J. A. Frieman, J. E. Gunn, L. Hui, B. Jain, D. Johnston, S. Kent, H. Lin, R. Nakajima, R. C. Nichol, J. P. Ostriker, A. Pope, R. Scranton, U. Seljak, R. K. Sheth, A. Stebbins, A. S. Szalay, I. Szapudi, Y. Xu, J. Annis, J. Brinkmann, S. Burles, F. J. Castander, I. Csabai, J. Loveday, M. Doi, M. Fukugita, B. Gillespie, G. Hennessy, D. W. Hogg, Ž. Ivezić, G. R. Knapp, D. Q. Lamb, B. C. Lee, R. H. Lupton, T. A. McKay, P. Kunszt, J. A. Munn,

- L. O’Connell, J. Peoples, J. R. Pier, M. Richmond, C. Rockosi, D. P. Schneider, C. Stoughton, D. L. Tucker, D. E. vanden Berk, B. Yanny, and D. G. York, *Cosmological parameters from SDSS and WMAP*, Phys. Rev. D **69** (May, 2004) 103501, [[astro-ph/](#)].
- [3] M. Tegmark, D. J. Eisenstein, M. A. Strauss, D. H. Weinberg, M. R. Blanton, J. A. Frieman, M. Fukugita, J. E. Gunn, A. J. S. Hamilton, G. R. Knapp, R. C. Nichol, J. P. Ostriker, N. Padmanabhan, W. J. Percival, D. J. Schlegel, D. P. Schneider, R. Scoccimarro, U. Seljak, H.-J. Seo, M. Swanson, A. S. Szalay, M. S. Vogeley, J. Yoo, I. Zehavi, K. Abazajian, S. F. Anderson, J. Annis, N. A. Bahcall, B. Bassett, A. Berlind, J. Brinkmann, T. Budavari, F. Castander, A. Connolly, I. Csabai, M. Doi, D. P. Finkbeiner, B. Gillespie, K. Glazebrook, G. S. Hennessey, D. W. Hogg, Ž. Ivezić, B. Jain, D. Johnston, S. Kent, D. Q. Lamb, B. C. Lee, H. Lin, J. Loveday, R. H. Lupton, J. A. Munn, K. Pan, C. Park, J. Peoples, J. R. Pier, A. Pope, M. Richmond, C. Rockosi, R. Scranton, R. K. Sheth, A. Stebbins, C. Stoughton, I. Szapudi, D. L. Tucker, D. E. vanden Berk, B. Yanny, and D. G. York, *Cosmological constraints from the SDSS luminous red galaxies*, Phys. Rev. D **74** (Dec., 2006) 123507, [[astro-ph/](#)].
- [4] S. Cole, W. J. Percival, J. A. Peacock, P. Norberg, C. M. Baugh, C. S. Frenk, I. Baldry, J. Bland-Hawthorn, T. Bridges, R. Cannon, M. Colless, C. Collins, W. Couch, N. J. G. Cross, G. Dalton, V. R. Eke, R. De Propris, S. P. Driver, G. Efstathiou, R. S. Ellis, K. Glazebrook, C. Jackson, A. Jenkins, O. Lahav, I. Lewis, S. Lumsden, S. Maddox, D. Madgwick, B. A. Peterson, W. Sutherland, and K. Taylor, *The 2dF Galaxy Redshift Survey: power-spectrum analysis of the final data set and cosmological implications*, MNRAS **362** (Sept., 2005) 505–534, [[astro-ph/](#)].
- [5] M. Davis, G. Efstathiou, C. S. Frenk, and S. D. M. White, *The evolution of large-scale structure in a universe dominated by cold dark matter*, ApJ **292** (May, 1985) 371–394.
- [6] A. Dekel and J. Silk, *The origin of dwarf galaxies, cold dark matter, and biased galaxy formation*, ApJ **303** (Apr., 1986) 39–55.
- [7] V. Trimble, *Existence and nature of dark matter in the universe*, ARA&A **25** (1987) 425–472.
- [8] C. S. Frenk, S. D. M. White, M. Davis, and G. Efstathiou, *The formation of dark halos in a universe dominated by cold dark matter*, ApJ **327** (Apr., 1988) 507–525.
- [9] A. Jenkins, C. S. Frenk, F. R. Pearce, P. A. Thomas, J. M. Colberg, S. D. M. White, H. M. P. Couchman, J. A. Peacock, G. Efstathiou, and A. H. Nelson, *Evolution of Structure in Cold Dark Matter Universes*, ApJ **499** (May, 1998) 20, [[astro-ph/](#)].
- [10] N. Arkani-Hamed, D. P. Finkbeiner, T. R. Slatyer, and N. Weiner, *A theory of dark matter*, Phys. Rev. D **79** (Jan., 2009) 015014, [[arXiv:0810.0713](#)].
- [11] H. J. Mo and S. D. M. White, *An analytic model for the spatial clustering of dark matter haloes*, MNRAS **282** (Sept., 1996) 347–361, [[astro-ph/](#)].
- [12] N. A. Bahcall, *Large-scale structure in the universe indicated by galaxy clusters*, ARA&A **26** (1988) 631–686.
- [13] R. E. Smith, J. A. Peacock, A. Jenkins, S. D. M. White, C. S. Frenk, F. R. Pearce, P. A. Thomas, G. Efstathiou, and H. M. P. Couchman, *Stable clustering, the halo model and non-linear cosmological power spectra*, MNRAS **341** (June, 2003) 1311–1332, [[astro-ph/](#)].
- [14] D. J. Eisenstein and W. Hu, *Power Spectra for Cold Dark Matter and Its Variants*, ApJ **511** (Jan., 1999) 5–15, [[astro-ph/](#)].
- [15] C. M. Baugh, S. Cole, C. S. Frenk, and C. G. Lacey, *The Epoch of Galaxy Formation*, ApJ **498** (May, 1998) 504, [[astro-ph/](#)].
- [16] N. Kaiser and G. Squires, *Mapping the dark matter with weak gravitational lensing*, ApJ **404** (Feb., 1993) 441–450.
- [17] R. K. Sheth and R. van de Weygaert, *A hierarchy of voids: much ado about nothing*, MNRAS **350** (May, 2004) 517–538, [[astro-ph/](#)].

- [18] J. R. Bond, L. Kofman, and D. Pogosyan, *How filaments of galaxies are woven into the cosmic web*, *Nature* **380** (Apr., 1996) 603–606, [[astro-ph/](#)].
- [19] R. van de Weygaert and W. Schaap, *The Cosmic Web: Geometric Analysis*, in *Data Analysis in Cosmology* (V. J. Martínez, E. Saar, E. Martínez-González, and M.-J. Pons-Bordería, eds.), vol. 665 of *Lecture Notes in Physics*, Berlin Springer Verlag, pp. 291–413, 2009.
- [20] J. A. Kesselman, A. Nusser, and P. J. E. Peebles, *Cosmology with equivalence principle breaking in the dark sector*, *Phys. Rev. D* **81** (Mar., 2010) 063521, [[arXiv:0912.4177](#)].
- [21] P. J. E. Peebles and A. Nusser, *Nearby galaxies as pointers to a better theory of cosmic evolution*, *Nature* **465** (June, 2010) 565–569, [[arXiv:1001.1484](#)].
- [22] P. J. E. Peebles, *The Void Phenomenon*, *Astrophys. J.* **557** (Aug., 2001) 495–504, [[astro-ph/](#)].
- [23] S. S. Gubser and P. J. E. Peebles, *Structure formation in a string-inspired modification of the cold dark matter model*, *Phys. Rev. D* **70** (Dec., 2004) 123510, [[hep-th/04](#)].
- [24] S. S. Gubser and P. J. E. Peebles, *Cosmology with a dynamically screened scalar interaction in the dark sector*, *Phys. Rev. D* **70** (Dec., 2004) 123511, [[hep-th/04](#)].
- [25] G. R. Farrar and P. J. E. Peebles, *Interacting Dark Matter and Dark Energy*, *Astrophys. J.* **604** (Mar., 2004) 1–11, [[astro-ph/0307316](#)].
- [26] G. R. Farrar and R. A. Rosen, *A New Force in the Dark Sector?*, *Phys. Rev. Lett.* **98** (Apr., 2007) 171302, [[astro-ph/0610298](#)].
- [27] A. Nusser, S. S. Gubser, and P. J. Peebles, *Structure formation with a long-range scalar dark matter interaction*, *Phys. Rev. D* **71** (Apr., 2005) 083505, [[astro-ph/0412586](#)].
- [28] W. A. Hellwing and R. Juszkiewicz, *Dark matter gravitational clustering with a long-range scalar interaction*, *Phys. Rev. D* **80** (Oct., 2009) 083522, [[arXiv:0809.1976](#)].
- [29] W. A. Hellwing, *Galactic halos in cosmology with long-range scalar DM interaction*, *Annalen der Physik* **19** (2010), no. 3-5 351–354, [[arXiv:0911.0573](#)].
- [30] W. A. Hellwing, S. R. Knollmann, and A. Knebe, *Boosting hierarchical structure formation with scalar-interacting dark matter*, *MNRAS* **408** (Oct., 2010) L104–L108, [[arXiv:1004.2929](#)].
- [31] R. Cen, *Cosmological reionization in LCDM models with and without a scalar field*, *New Astronomy Review* **50** (Mar., 2006) 191–198.
- [32] W. A. Hellwing, R. Juszkiewicz, and R. van de Weygaert, *Hierarchy of N -point functions in the Λ CDM and ReBEL cosmologies*, *Phys. Rev. D* **82** (Nov., 2010) 103536, [[arXiv:1008.3930](#)].
- [33] M. Baldi, V. Pettorino, G. Robbers, and V. Springel, *Hydrodynamical N -body simulations of coupled dark energy cosmologies*, *MNRAS* **403** (Apr., 2010) 1684–1702, [[arXiv:0812.3901](#)].
- [34] M. Baldi, *Simulations of structure formation in interacting dark energy cosmologies*, *Nuclear Physics B Proceedings Supplements* **194** (Oct., 2009) 178–184, [[arXiv:0906.5353](#)].
- [35] M. Baldi and P. Salucci, *Constraints on interacting Dark Energy models from galaxy rotation curves*, *Journal of Cosmology and Astro-Particle Physics* **2** (Feb., 2012) 14, [[arXiv:1111.3953](#)].
- [36] B. Li and J. D. Barrow, *On the effects of coupled scalar fields on structure formation*, *MNRAS* **413** (May, 2011) 262–270, [[arXiv:1010.3748](#)].
- [37] B. Li, *Voids in coupled scalar field cosmology*, *MNRAS* **411** (Mar., 2011) 2615–2627, [[arXiv:1009.1406](#)].
- [38] B. Li, D. F. Mota, and J. D. Barrow, *N -body Simulations for Extended Quintessence Models*, *ApJ* **728** (Feb., 2011) 109, [[arXiv:1009.1400](#)].
- [39] B. Li and J. D. Barrow, *N -body simulations for coupled scalar-field cosmology*, *Phys. Rev. D* **83** (Jan., 2011) 024007, [[arXiv:1005.4231](#)].

- [40] M. Baldi, *Clarifying the effects of interacting dark energy on linear and non-linear structure formation processes*, *MNRAS* **414** (June, 2011) 116–128, [[arXiv:1012.0002](#)].
- [41] M. Baldi, *Time-dependent couplings in the dark sector: from background evolution to non-linear structure formation*, *MNRAS* **411** (Feb., 2011) 1077–1103, [[arXiv:1005.2188](#)].
- [42] A.-C. Davis, B. Li, D. F. Mota, and H. A. Winther, *Structure Formation in the Symmetron Model*, *ArXiv e-prints* (Aug., 2011) [[arXiv:1108.3081](#)].
- [43] M. Baldi, *Early massive clusters and the bouncing coupled dark energy*, *ArXiv e-prints* (July, 2011) [[arXiv:1107.5049](#)].
- [44] M. Baldi, J. Lee, and A. V. Macciò, *The Effect of Coupled Dark Energy on the Alignment Between Dark Matter and Galaxy Distributions in Clusters*, *ApJ* **732** (May, 2011) 112, [[arXiv:1101.5761](#)].
- [45] B. Li and H. Zhao, *Structure formation by the fifth force: Segregation of baryons and dark matter*, *Phys. Rev. D* **81** (May, 2010) 104047, [[arXiv:1001.3152](#)].
- [46] H. Zhao, A. V. Macciò, B. Li, H. Hoekstra, and M. Feix, *Structure Formation by Fifth Force: Power Spectrum from N-Body Simulations*, *ApJ* **712** (Apr., 2010) L179–L183, [[arXiv:0910.3207](#)].
- [47] B. Li, W. A. Hellwing, K. Koyama, G.-B. Zhao, E. Jennings, and C. M. Baugh, *The non-linear matter and velocity power spectra in $f(R)$ gravity*, *MNRAS* **428** (Jan., 2013) 743–755, [[arXiv:1206.4317](#)].
- [48] H. Shan, B. Qin, B. Fort, C. Tao, X.-P. Wu, and H. Zhao, *Offset between dark matter and ordinary matter: evidence from a sample of 38 lensing clusters of galaxies*, *MNRAS* **406** (Aug., 2010) 1134–1139, [[arXiv:1004.1475](#)].
- [49] A. M. Swinbank and et al., *The discovery of a massive supercluster at $z = 0.9$ in the UKIDSS Deep eXtragalactic Survey*, *MNRAS* **379** (Aug., 2007) 1343–1351, [[arXiv:0706.0090](#)].
- [50] R. J. Foley, K. Andersson, G. Bazin, T. de Haan, J. Ruel, P. A. R. Ade, K. A. Aird, R. Armstrong, M. L. N. Ashby, M. Bautz, B. A. Benson, L. E. Bleem, M. Bonamente, M. Brodwin, J. E. Carlstrom, C. L. Chang, A. Clocchiatti, T. M. Crawford, A. T. Crites, S. Desai, M. A. Dobbs, J. P. Dudley, G. G. Fazio, W. R. Forman, G. Garmire, E. M. George, M. D. Gladders, A. H. Gonzalez, N. W. Halverson, F. W. High, G. P. Holder, W. L. Holzapfel, S. Hoover, J. D. Hrubes, C. Jones, M. Joy, R. Keisler, L. Knox, A. T. Lee, E. M. Leitch, M. Lueker, D. Luong-Van, D. P. Marrone, J. J. McMahon, J. Mehl, S. S. Meyer, J. J. Mohr, T. E. Montroy, S. S. Murray, S. Padin, T. Plagge, C. Pryke, C. L. Reichardt, A. Rest, J. E. Ruhl, B. R. Saliwanchik, A. Saro, K. K. Schaffer, L. Shaw, E. Shirokoff, J. Song, H. G. Spieler, B. Stalder, S. A. Stanford, Z. Staniszewski, A. A. Stark, K. Story, C. W. Stubbs, K. Vanderlinde, J. D. Vieira, A. Vikhlinin, R. Williamson, and A. Zenteno, *Discovery and Cosmological Implications of SPT-CL J2106-5844, the Most Massive Known Cluster at $z \approx 1$* , *ApJ* **731** (Apr., 2011) 86, [[arXiv:1101.1286](#)].
- [51] M. Brodwin, J. Ruel, P. A. R. Ade, K. A. Aird, K. Andersson, M. L. N. Ashby, M. Bautz, G. Bazin, B. A. Benson, L. E. Bleem, J. E. Carlstrom, C. L. Chang, T. M. Crawford, A. T. Crites, T. de Haan, S. Desai, M. A. Dobbs, J. P. Dudley, G. G. Fazio, R. J. Foley, W. R. Forman, G. Garmire, E. M. George, M. D. Gladders, A. H. Gonzalez, N. W. Halverson, F. W. High, G. P. Holder, W. L. Holzapfel, J. D. Hrubes, C. Jones, M. Joy, R. Keisler, L. Knox, A. T. Lee, E. M. Leitch, M. Lueker, D. P. Marrone, J. J. McMahon, J. Mehl, S. S. Meyer, J. J. Mohr, T. E. Montroy, S. S. Murray, S. Padin, T. Plagge, C. Pryke, C. L. Reichardt, A. Rest, J. E. Ruhl, K. K. Schaffer, L. Shaw, E. Shirokoff, J. Song, H. G. Spieler, B. Stalder, S. A. Stanford, Z. Staniszewski, A. A. Stark, C. W. Stubbs, K. Vanderlinde, J. D. Vieira, A. Vikhlinin, R. Williamson, Y. Yang, O. Zahn, and A. Zenteno, *SPT-CL J0546-5345: A Massive $z \approx 1$ Galaxy Cluster Selected Via the Sunyaev-Zel'dovich Effect with the South Pole Telescope*, *ApJ* **721** (Sept., 2010) 90–97, [[arXiv:1006.5639](#)].
- [52] E. Carlesi, A. Knebe, G. Yepes, S. Gottloeber, J. Beltran Jimenez, and A. L. Maroto, *Vector dark energy and high- z massive clusters*, *ArXiv e-prints* (Aug., 2011) [[arXiv:1108.4173](#)].
- [53] M. Baldi and V. Pettorino, *High- z massive clusters as a test for dynamical coupled dark energy*,

MNRAS **412** (Mar., 2011) L1–L5, [[arXiv:1006.3761](#)].

- [54] M. J. Mortonson, W. Hu, and D. Huterer, *Simultaneous falsification of Λ CDM and quintessence with massive, distant clusters*, *Phys. Rev. D* **83** (Jan., 2011) 023015, [[arXiv:1011.0004](#)].
- [55] G. Nordström, *Zur Theorie der Gravitation vom Standpunkt des Relativitätsprinzips*, *Annalen der Physik* **347** (1913) 533–554.
- [56] H. Yukawa, *On the Interaction of Elementary Particles*, *Proceedings of the Physico-Mathematical Society of Japan* **17** (1935) 48–57.
- [57] R. H. Dicke, *Scalar-Tensor Gravitation and the Cosmic Fireball*, *ApJ* **152** (Apr., 1968) 1.
- [58] R. H. Dicke, *Long-Range Scalar Interaction*, *Physical Review* **126** (June, 1962) 1875–1877.
- [59] P. Jordan, *Zum gegenwärtigen Stand der Diracschen kosmologischen Hypothesen*, *Zeitschrift für Physik* **157** (Feb., 1959) 112–121.
- [60] T. Damour, G. W. Gibbons, and C. Gundlach, *Dark matter, time-varying G , and a dilaton field*, *Physical Review Letters* **64** (Jan., 1990) 123–126.
- [61] B.-A. Gradwohl and J. A. Frieman, *Dark matter, long-range forces, and large-scale structure*, *Astrophys. J.* **398** (Oct., 1992) 407–424.
- [62] J. A. Frieman and B.-A. Gradwohl, *Dark matter and the equivalence principle*, *Physical Review Letters* **67** (Nov., 1991) 2926–2929.
- [63] J. A. Casas, J. Garcia-Bellido, and M. Quiros, *Scalar-tensor theories of gravity with Φ -dependent masses*, *Classical and Quantum Gravity* **9** (May, 1992) 1371–1384, [[hep-ph/92](#)].
- [64] T. Damour and A. M. Polyakov, *String theory and gravity*, *General Relativity and Gravitation* **26** (Dec., 1994) 1171–1176, [[gr-qc/941](#)].
- [65] C. Wetterich, *An asymptotically vanishing time-dependent cosmological "constant"*, *A&A* **301** (Sept., 1995) 321, [[hep-th/94](#)].
- [66] G. W. Anderson and S. M. Carroll, *Dark Matter with Time-Dependent Mass*, in *COSMO-97, First International Workshop on Particle Physics and the Early Universe* (L. Roszkowski, ed.), p. 227, 1998.
- [67] R. Bean, *Perturbation evolution with a nonminimally coupled scalar field*, *Phys. Rev. D* **64** (Dec., 2001) 123516, [[astro-ph/0104464](#)].
- [68] L. Amendola, *Perturbations in a coupled scalar field cosmology*, *MNRAS* **312** (Mar., 2000) 521–530, [[astro-ph/9906073](#)].
- [69] L. Amendola and D. Tocchini-Valentini, *Baryon bias and structure formation in an accelerating universe*, *Phys. Rev. D* **66** (Aug., 2002) 043528, [[astro-ph/0111535](#)].
- [70] U. França and R. Rosenfeld, *Fine Tuning in Quintessence Models with Exponential Potentials*, *Journal of High Energy Physics* **10** (Oct., 2002) 15, [[astro-ph/0206194](#)].
- [71] T. Damour, F. Piazza, and G. Veneziano, *Violations of the equivalence principle in a dilaton-runaway scenario*, *Phys. Rev. D* **66** (Aug., 2002) 046007, [[hep-th/02](#)].
- [72] D. Comelli, M. Pietroni, and A. Riotto, *Dark energy and dark matter*, *Physics Letters B* **571** (Oct., 2003) 115–120, [[hep-ph/03](#)].
- [73] L. Amendola, M. Gasperini, and F. Piazza, *Fitting type Ia supernovae with coupled dark energy*, *Journal of Cosmology and Astro-Particle Physics* **9** (Sept., 2004) 14, [[astro-ph/0407573](#)].
- [74] A. W. Brookfield, C. van de Bruck, and L. M. H. Hall, *New interactions in the dark sector mediated by dark energy*, *Phys. Rev. D* **77** (Feb., 2008) 043006, [[arXiv:0709.2297](#)].
- [75] M. Baldi, *Structure formation in multiple dark matter cosmologies with long-range scalar interactions*, *MNRAS* **428** (Jan., 2013) 2074–2084, [[arXiv:1206.2348](#)].
- [76] M. Baldi, *Cosmological models with multiple dark matter species and long-range scalar interactions*,

ArXiv e-prints (Apr., 2013) [[arXiv:1304.5178](#)].

- [77] M. Baldi, *Multiple dark matter as a self-regulating mechanism for dark sector interactions*, *Annalen der Physik* **524** (Oct., 2012) 602–617, [[arXiv:1204.0514](#)].
- [78] P. J. E. Peebles, *The large-scale structure of the universe*. Research supported by the National Science Foundation. Princeton, N.J., Princeton University Press, 1980. 435 p., 1980.
- [79] W. A. Hellwing, B. Li, C. S. Frenk, and S. Cole, *Hierarchical clustering in chameleon $f(R)$ gravity*, *ArXiv e-prints* (May, 2013) [[arXiv:1305.7486](#)].
- [80] V. Springel, *The cosmological simulation code GADGET-2*, *MNRAS* **364** (Dec., 2005) 1105–1134, [[astro-ph/0505010](#)].
- [81] S. P. D. Gill, A. Knebe, and B. K. Gibson, *The evolution of substructure - I. A new identification method*, *MNRAS* **351** (June, 2004) 399–409, [[astro-ph/0404258](#)].
- [82] S. R. Knollmann and A. Knebe, *AHF: Amiga’s Halo Finder*, *ApJS* **182** (June, 2009) 608–624, [[arXiv:0904.3662](#)].
- [83] S. D. M. White and M. J. Rees, *Core condensation in heavy halos - A two-stage theory for galaxy formation and clustering*, *MNRAS* **183** (May, 1978) 341–358.
- [84] D. J. Croton, V. Springel, S. D. M. White, G. De Lucia, C. S. Frenk, L. Gao, A. Jenkins, G. Kauffmann, J. F. Navarro, and N. Yoshida, *The many lives of active galactic nuclei: cooling flows, black holes and the luminosities and colours of galaxies*, *MNRAS* **365** (Jan., 2006) 11–28, [[astro-ph/](#)].
- [85] S. D. M. White and C. S. Frenk, *Galaxy formation through hierarchical clustering*, *ApJ* **379** (Sept., 1991) 52–79.
- [86] G. R. Blumenthal, S. M. Faber, R. Flores, and J. R. Primack, *Contraction of dark matter galactic halos due to baryonic infall*, *ApJ* **301** (Feb., 1986) 27–34.
- [87] D. H. Rudd, A. R. Zentner, and A. V. Kravtsov, *Effects of Baryons and Dissipation on the Matter Power Spectrum*, *ApJ* **672** (Jan., 2008) 19–32, [[astro-ph/](#)].
- [88] T. Sawala, C. S. Frenk, R. A. Crain, A. Jenkins, J. Schaye, T. Theuns, and J. Zavala, *The abundance of (not just) dark matter haloes*, *MNRAS* **431** (May, 2013) 1366–1382, [[arXiv:1206.6495](#)].
- [89] M. Kesden and M. Kamionkowski, *Tidal tails test the equivalence principle in the dark-matter sector*, *Phys. Rev. D* **74** (Oct., 2006) 083007, [[astro-ph/](#)].
- [90] J. A. Kesselman, A. Nusser, and P. J. E. Peebles, *Galaxy satellites and the weak equivalence principle*, *Phys. Rev. D* **80** (Sept., 2009) 063517, [[arXiv:0902.3452](#)].
- [91] E. Puchwein, M. Baldi, and V. Springel, *Modified Gravity-GADGET: A new code for cosmological hydrodynamical simulations of modified gravity models*, *ArXiv e-prints* (May, 2013) [[arXiv:1305.2418](#)].
- [92] J. F. Navarro, C. S. Frenk, and S. D. M. White, *A Universal Density Profile from Hierarchical Clustering*, *ApJ* **490** (Dec., 1997) 493, [[astro-ph/9611107](#)].
- [93] R. H. Wechsler, J. S. Bullock, J. R. Primack, A. V. Kravtsov, and A. Dekel, *Concentrations of Dark Halos from Their Assembly Histories*, *Astrophys. J.* **568** (Mar., 2002) 52–70, [[astro-ph/0108151](#)].
- [94] M. Boylan-Kolchin, J. S. Bullock, and M. Kaplinghat, *The Milky Way’s bright satellites as an apparent failure of Λ CDM*, *MNRAS* **422** (May, 2012) 1203–1218, [[arXiv:1111.2048](#)].
- [95] M. Boylan-Kolchin, J. S. Bullock, and M. Kaplinghat, *Too big to fail? The puzzling darkness of massive Milky Way subhaloes*, *MNRAS* **415** (July, 2011) L40–L44, [[arXiv:1103.0007](#)].
- [96] J. Wang, C. S. Frenk, J. F. Navarro, L. Gao, and T. Sawala, *The missing massive satellites of the Milky Way*, *MNRAS* **424** (Aug., 2012) 2715–2721, [[arXiv:1203.4097](#)].

- [97] F. Hoyle, *The Origin of the Rotations of the Galaxies*, in *Problems of Cosmical Aerodynamics*, p. 195, 1951.
- [98] P. J. E. Peebles, *Origin of the Angular Momentum of Galaxies*, *ApJ* **155** (Feb., 1969) 393.
- [99] A. G. Doroshkevich, *The space structure of perturbations and the origin of rotation of galaxies in the theory of fluctuation.*, *Astrofizika* **6** (1970) 581–600.
- [100] G. Efstathiou and B. J. T. Jones, *The rotation of galaxies - Numerical investigations of the tidal torque theory*, *MNRAS* **186** (Jan., 1979) 133–144.
- [101] S. M. Fall and G. Efstathiou, *Formation and rotation of disc galaxies with haloes*, *MNRAS* **193** (Oct., 1980) 189–206.
- [102] S. D. M. White, *Angular momentum growth in protogalaxies*, *ApJ* **286** (Nov., 1984) 38–41.
- [103] P. J. E. Peebles, *Origin of the Angular Momentum of Galaxies*, *ApJ* **155** (Feb., 1969) 393.
- [104] M. Vitvitska, A. A. Klypin, A. V. Kravtsov, R. H. Wechsler, J. R. Primack, and J. S. Bullock, *The Origin of Angular Momentum in Dark Matter Halos*, *ApJ* **581** (Dec., 2002) 799–809, [[astro-ph/](#)].
- [105] J. Barnes and G. Efstathiou, *Angular momentum from tidal torques*, *ApJ* **319** (Aug., 1987) 575–600.
- [106] M. S. Warren, P. J. Quinn, J. K. Salmon, and W. H. Zurek, *Dark halos formed via dissipationless collapse. I - Shapes and alignment of angular momentum*, *ApJ* **399** (Nov., 1992) 405–425.
- [107] B. Robertson, J. S. Bullock, T. J. Cox, T. Di Matteo, L. Hernquist, V. Springel, and N. Yoshida, *A Merger-driven Scenario for Cosmological Disk Galaxy Formation*, *ApJ* **645** (July, 2006) 986–1000, [[astro-ph/](#)].
- [108] J. S. Bullock, A. Dekel, T. S. Kolatt, A. V. Kravtsov, A. A. Klypin, C. Porciani, and J. R. Primack, *A Universal Angular Momentum Profile for Galactic Halos*, *Astrophys. J.* **555** (July, 2001) 240–257, [[astro-ph/0011001](#)].
- [109] M. S. Warren, P. J. Quinn, J. K. Salmon, and W. H. Zurek, *Dark halos formed via dissipationless collapse. I - Shapes and alignment of angular momentum*, *ApJ* **399** (Nov., 1992) 405–425.
- [110] S. Cole and C. Lacey, *The structure of dark matter haloes in hierarchical clustering models*, *MNRAS* **281** (July, 1996) 716, [[astro-ph/9510147](#)].
- [111] H. J. Mo, S. Mao, and S. D. M. White, *The formation of galactic discs*, *MNRAS* **295** (Apr., 1998) 319–336, [[astro-ph/9707093](#)].
- [112] M. Steinmetz and M. Bartelmann, *On the spin parameter of dark-matter haloes*, *MNRAS* **272** (Feb., 1995) 570–578, [[astro-ph/9403017](#)].
- [113] P. Catelan and T. Theuns, *Evolution of the angular momentum of protogalaxies from tidal torques: Zel’dovich approximation*, *MNRAS* **282** (Sept., 1996) 436–454, [[astro-ph/9604077](#)].
- [114] F. Governato, B. Willman, L. Mayer, A. Brooks, G. Stinson, O. Valenzuela, J. Wadsley, and T. Quinn, *Forming disc galaxies in Λ CDM simulations*, *MNRAS* **374** (Feb., 2007) 1479–1494, [[astro-ph/0602351](#)].
- [115] B. Robertson, J. S. Bullock, T. J. Cox, T. Di Matteo, L. Hernquist, V. Springel, and N. Yoshida, *A Merger-driven Scenario for Cosmological Disk Galaxy Formation*, *ApJ* **645** (July, 2006) 986–1000, [[astro-ph/0503369](#)].
- [116] A. V. Macciò, A. A. Dutton, F. C. van den Bosch, B. Moore, D. Potter, and J. Stadel, *Concentration, spin and shape of dark matter haloes: scatter and the dependence on mass and environment*, *MNRAS* **378** (June, 2007) 55–71, [[astro-ph/0608157](#)].
- [117] P. Bett, V. Eke, C. S. Frenk, A. Jenkins, J. Helly, and J. Navarro, *The spin and shape of dark matter haloes in the Millennium simulation of a Λ cold dark matter universe*, *MNRAS* **376** (Mar., 2007) 215–232, [[astro-ph/0608607](#)].

- [118] A. Knebe and C. Power, *On the Correlation between Spin Parameter and Halo Mass*, ApJ **678** (May, 2008) 621–626, [[arXiv:0801.4453](#)].
- [119] J. M. Bardeen, J. R. Bond, N. Kaiser, and A. S. Szalay, *The statistics of peaks of Gaussian random fields*, ApJ **304** (May, 1986) 15–61.
- [120] J. R. Bond and S. T. Myers, *The Peak-Patch Picture of Cosmic Catalogs. I. Algorithms*, ApJS **103** (Mar., 1996) 1.
- [121] R. van de Weygaert and E. Bertschinger, *Peak and gravity constraints in Gaussian primordial density fields: An application of the Hoffman-Ribak method*, MNRAS **281** (July, 1996) 84, [[astro-ph/9507024](#)].
- [122] R. K. Sheth, H. J. Mo, and G. Tormen, *Ellipsoidal collapse and an improved model for the number and spatial distribution of dark matter haloes*, MNRAS **323** (May, 2001) 1–12, [[astro-ph/9907024](#)].
- [123] J. R. Bond, L. Kofman, and D. Pogosyan, *How filaments of galaxies are woven into the cosmic web*, Nature **380** (Apr., 1996) 603–606, [[astro-ph/9512141](#)].
- [124] R. van de Weygaert, *Clusters and the Cosmic Web*, ArXiv Astrophysics e-prints (July, 2006) [[astro-ph/0607539](#)].
- [125] M. van Haarlem and R. van de Weygaert, *Velocity Fields and Alignments of Clusters in Gravitational Instability Scenarios*, ApJ **418** (Dec., 1993) 544.
- [126] M. Franx, G. Illingworth, and T. de Zeeuw, *The ordered nature of elliptical galaxies - Implications for their intrinsic angular momenta and shapes*, ApJ **383** (Dec., 1991) 112–134.
- [127] L. D. Shaw, J. Weller, J. P. Ostriker, and P. Bode, *Statistics of Physical Properties of Dark Matter Clusters*, ApJ **646** (Aug., 2006) 815–833, [[astro-ph/](#)].
- [128] C. Power, A. Knebe, and S. R. Knollmann, *The dynamical state of dark matter haloes in cosmological simulations - I. Correlations with mass assembly history*, MNRAS (Oct., 2011) 1734, [[arXiv:1109.2671](#)].
- [129] G. Gentile, P. Salucci, U. Klein, D. Vergani, and P. Kalberla, *The cored distribution of dark matter in spiral galaxies*, MNRAS **351** (July, 2004) 903–922, [[astro-ph/](#)].
- [130] T. Broadhurst, N. Benítez, D. Coe, K. Sharon, K. Zekser, R. White, H. Ford, R. Bouwens, J. Blakeslee, M. Clampin, N. Cross, M. Franx, B. Frye, G. Hartig, G. Illingworth, L. Infante, F. Menanteau, G. Meurer, M. Postman, D. R. Ardila, F. Bartko, R. A. Brown, C. J. Burrows, E. S. Cheng, P. D. Feldman, D. A. Golimowski, T. Goto, C. Gronwall, D. Herranz, B. Holden, N. Homeier, J. E. Krist, M. P. Lesser, A. R. Martel, G. K. Miley, P. Rosati, M. Sirianni, W. B. Sparks, S. Steindling, H. D. Tran, Z. I. Tsvetanov, and W. Zheng, *Strong-Lensing Analysis of A1689 from Deep Advanced Camera Images*, ApJ **621** (Mar., 2005) 53–88, [[astro-ph/](#)].
- [131] J. D. Simon, A. D. Bolatto, A. Leroy, L. Blitz, and E. L. Gates, *High-Resolution Measurements of the Halos of Four Dark Matter-Dominated Galaxies: Deviations from a Universal Density Profile*, ApJ **621** (Mar., 2005) 757–776, [[astro-ph/](#)].
- [132] J. Diemand, M. Zemp, B. Moore, J. Stadel, and C. M. Carollo, *Cusps in cold dark matter haloes*, MNRAS **364** (Dec., 2005) 665–673, [[astro-ph/](#)].
- [133] L. E. Strigari, J. S. Bullock, M. Kaplinghat, J. Diemand, M. Kuhlen, and P. Madau, *Redefining the Missing Satellites Problem*, ApJ **669** (Nov., 2007) 676–683, [[arXiv:0704.1817](#)].
- [134] G. Gentile, A. Burkert, P. Salucci, U. Klein, and F. Walter, *The Dwarf Galaxy DDO 47 as a Dark Matter Laboratory: Testing Cusps Hiding in Triaxial Halos*, ApJ **634** (Dec., 2005) L145–L148, [[astro-ph/](#)].
- [135] E. Hayashi, J. F. Navarro, C. Power, A. Jenkins, C. S. Frenk, S. D. M. White, V. Springel, J. Stadel, and T. R. Quinn, *The inner structure of Λ CDM haloes - II. Halo mass profiles and low surface brightness galaxy rotation curves*, MNRAS **355** (Dec., 2004) 794–812, [[astro-ph/](#)].

- [136] A. A. El-Zant, Y. Hoffman, J. Primack, F. Combes, and I. Shlosman, *Flat-cored Dark Matter in Cuspy Clusters of Galaxies*, ApJ **607** (June, 2004) L75–L78, [[astro-ph/](#)].
- [137] J. Diemand, M. Kuhlen, P. Madau, M. Zemp, B. Moore, D. Potter, and J. Stadel, *Clumps and streams in the local dark matter distribution*, Nature **454** (Aug., 2008) 735–738, [[arXiv:0805.1244](#)].
- [138] B. Li and J. D. Barrow, *N-Body Simulations for Coupled Scalar Field Cosmology*, ArXiv e-prints (May, 2010) [[arXiv:1005.4231](#)].
- [139] B. Li, G.-B. Zhao, and K. Koyama, *Haloes and voids in $f(R)$ gravity*, MNRAS **421** (Apr., 2012) 3481–3487, [[arXiv:1111.2602](#)].
- [140] H. A. Winther, D. F. Mota, and B. Li, *Environment Dependence of Dark Matter Halos in Symmetron Modified Gravity*, ApJ **756** (Sept., 2012) 166, [[arXiv:1110.6438](#)].